POWER EFFICIENT WIRELESS SENSORS FOR GAS CONCENTRATION MEASUREMENT

BY

HAMZA SHAHID

A Thesis Presented to the
DEANSHIP OF GRADUATE STUDIES

KING FAHD UNIVERSITY OF PETROLEUM & MINERALS

DHAHRAN, SAUDI ARABIA

In Partial Fulfillment of the
Requirements for the Degree of

MASTER OF SCIENCE

In

ELECTRICAL ENGINEERING

April 2017

KING FAHD UNIVERSITY OF PETROLEUM & MINERALS

DHAHRAN- 31261, SAUDI ARABIA

DEANSHIP OF GRADUATE STUDIES

This thesis, written by **Hamza Shahid** under the direction his thesis advisor and approved by his thesis committee, has been presented and accepted by the Dean of Graduate Studies, in partial fulfillment of the requirements for the degree of **MASTER OF SCIENCE IN ELECTRICAL ENGINEERING.**

Dr. Hussain Abdullah Alzaher
(Advisor)

Dr. Ali Ahmad Al-Shaikhi
Department Chairman

Dr. Mohammad K. Alghamdi
(Member)

Dr. Salam A. Zummo
Dean of Graduate Studies

Dr. Alaa El-Din Hussein
(Member)

22/5/17

Date

Dedicated to my parents and siblings

ACKNOWLEDGMENTS

All praise is due to ALLAH and peace be upon the Prophet ﷺ and his family, his companions (may ALLAH be pleased with them) and his followers.

Through utmost respect, I would like to share my inmost regards to my parents and my family, without their prayers, moral support and love, I would not have been able to accomplish my desired objectives in life. I will always be grateful to them for their constant prayers, support and inspiration.

It has been my honor to be able to work with Dr. Hussain Abdullah Alzaher. I would like to admire his supervision, suggestions and guidance right from the beginning till the end of this research. His constant motivation helps me to produce quality work. I would like to thank my committee members: Dr. Mohammad K. Alghamdi and Dr. Alaa El-Din Hussein for their useful response, advice and the time they spent reviewing this thesis. I am very obliged to King Fahd University of Petroleum & Minerals for providing me an opportunity to pursue my graduate degree.

TABLE OF CONTENTS

ACKNOWLEDGMENTS ..... **V**

TABLE OF CONTENTS ..... **VI**

LIST OF TABLES ..... **IX**

LIST OF FIGURES ..... **X**

LIST OF ABBREVIATIONS ..... **XII**

ABSTRACT ..... **XIV**

ملخص الرسالة ..... **XVI**

CHAPTER 1 INTRODUCTION **1**

1.1 Motivation **4**

1.2 Requirements from a sensor **5**

1.3 Thesis Objectives **6**

1.4 Thesis Methodology **6**

1.5 Thesis Contribution: **7**

1.6 Thesis Breakdown **8**

CHAPTER 2 LITERATURE REVIEW **9**

2.1 Background: **9**

2.2 Applications of Wireless Sensors: **10**

2.3 Classification of Gas sensors based upon method of sensing **11**

2.4 Evaluation of Gas Sensing Methods: **11**

2.5 Approaches for Metal Oxides semiconductor based Gas Sensors: **14**

2.6 Blocks of Wireless Gas Sensors: **15**

2.6.1 Sensor Front End: 16
2.6.2 Drawback of the approach: 17
2.6.3 Low Noise Amplifier: 18
2.6.4 Microcontroller: 20
2.6.5 Voltage/Current to frequency Converter: 24
CHAPTER 3 GAS SENSOR: INTEGRATED CIRCUIT APPROACH 27
3.1 Sub hertz Oscillator 28
3.1.1 The feedback loop 28
3.1.2 Relaxation Oscillator: 30
3.1.3 Proposed Oscillator: 32
3.2 Voltage Dividers 38
3.3 Buffer 39
3.4 Wheatstone bridge 40
3.4.1 Micro-heater for gas sensor 41
3.4.2 Noise analysis of Wheatstone bridge: 45
3.5 Oscillator for excitation of Wheatstone bridge 47
3.6 Analog Buffer 48
3.7 Difference Amplifier: 50
3.8 Switching Transistors 52
3.9 Operation during the presence of gas 53
CHAPTER 4 RESULTS AND DISCUSSIONS 55
4.1 Output of Sub Hertz Oscillator 55
4.2 Output at Buffer Stage 57
4.3 Characteristics of 1 KHz oscillator: 57

4.4 Characteristics of Analog Buffer Stage 59

4.5 Characteristics at Wheatstone bridge: 60

4.6 Output Characteristics of Gas Sensor: 61

4.7 Summary of the Results 74

4.8 Comparison with Other Sensors: 77

CHAPTER 5 POST LAYOUT SIMULATION 79

5.1 Layout for gas sensor circuit based on Schmitt Trigger based Timer. 79

5.2 Post Layout Simulations for both configuration of gas sensors 80

CHAPTER 6 CONCLUSION AND FUTURE WORK 82

6.1 Conclusion 82

6.2 Future Work: 83

REFERENCES 84

VITAE 91

LIST OF TABLES

Table 2.1 Advantages, disadvantages and applications of different Gas sensors 14
Table 2.2 Power Consumption comparison for different sensor circuits..... 26
Table 3.1 Sizes of the transistors in Oscillator 38
Table 3.2 Sizes of 1 KHz oscillator circuit 48
Table 3.3 Sizes for the Analog Buffer 49
Table 3.4 Sizes for the difference amplifier..... 52
Table 4.1 Summary for increase in Resistance of KΩ..... 74
Table 4.2 Summary of decrease of resistance in KΩ..... 75
Table 4.3 Summary of increase in resistance in MΩ..... 75
Table 4.4 Summary of decrease in resistance for MΩ..... 76
Table 4.5 State-of-the-art Gas Sensing Circuits: Comparative Study 78
Table 5.1 Comparison for both configurations 81

LIST OF FIGURES

Figure 1.1 Basic elements inside a general Sensor 2
Figure 2.1 General Applications of Wireless Sensors 10
Figure 2.2 Classification of Gas Sensing Methods 11
Figure 2.3 Approaches for Wireless Gas Sensors 15
Figure 2.4 Sensing front end circuits (a) Wheatstone (b) Voltage Divider 17
Figure 2.5 Typical application circuit for increased linearity. 19
Figure 2.6 Tri-level comparator SAR ADC architecture 22
Figure 2.7 Block diagram of frequency to digital converter 23
Figure 2.8 Sensor heating profiles with time 24
Figure 2.9 Circuit diagram of a voltage controlled ring oscillator.[3] 25
Figure 2.10 Schematic circuit for source coupled multi-vibrator 25
Figure 3.1 Flow diagram for the proposed sensor approach 27
Figure 3.2 Positive feedback loop for bi-stable operation 29
Figure 3.3 Bi-stable circuit with transfer characteristics 30
Figure 3.4 Astable Multivibrator 31
Figure 3.5 Proposed CMOS based Oscillator 33
Figure 3.6 CMOS based Schmitt Trigger 34
Figure 3.7 Voltage dividers for the circuit 39
Figure 3.8 Inverter based buffer 40
Figure 3.9 Wheatstone bridge configuration of sensor front-end 41
Figure 3.10 Typical micro-heater 42
Figure 3.11 Plate structure of micro-heater with hole in center 43
Figure 3.12 Meander line structure 43
Figure 3.13 Double Spiral Shaped 44
Figure 3.14 Fan shaped Micro-heater 44
Figure 3.15 Honey-comb Shaped Micro-heater 44
Figure 3.16 S-Shaped Micro-Heater 45
Figure 3.17 Noise spectrum for resistive circuit 46
Figure 3.18 1 KHz oscillator for Bridge excitation 47
Figure 3.19 Analog buffer based on two stage op-amp 49
Figure 3.20 Difference Amplifier 51
Figure 3.21 Transistor Switch 53
Figure 4.1 Output Characteristics of Sub-Hertz Oscillator with C=100p 56
Figure 4.2 Output Characteristics of Sub-Hertz Oscillator with C=50p 56
Figure 4.3 Output characteristics at buffer stage 57
Figure 4.4 Output of 1 KHz Oscillator 58
Figure 4.5 Zooming in the waveform of 1 KHz oscillator 58
Figure 4.6 Capacitor voltage for the 1 KHz oscillator 59
Figure 4.7 Output waveform of Analog buffer compared with capacitor voltage 59

Figure 4.8 Outputs of Wheatstone Bridge at equal transistors of 1KΩ 60
Figure 4.9 Outputs of Wheatstone Bridge at 1KΩ and 2KΩ resistors in one branch..... 61
Figure 4.10 Output for the case of both 1 KΩ Resistors..... 62
Figure 4.11 Output for the case of increase of 1% resistance..... 63
Figure 4.12 Output for the case of increase of 5% resistance..... 63
Figure 4.13 Output for the case of increase of 10% resistance..... 64
Figure 4.14 Output for the case of increase of 20% resistance..... 65
Figure 4.15 Output for the case of increase of 50% resistance..... 65
Figure 4.16 Output for the case of increase of 100% resistance..... 66
Figure 4.17 Output for the case of decrease of 5% resistance 67
Figure 4.18 Output for the case of decrease of 10% resistance 67
Figure 4.19 Output for the case 1MΩ - 1MΩ 68
Figure 4.20 Output for the case of increase of 1% resistance..... 69
Figure 4.21 Output for the case of increase of 5% resistance..... 70
Figure 4.22 Output for the case of increase of 10% resistance..... 70
Figure 4.23 Output for the case of increase of 20% resistance..... 71
Figure 4.24 Output for the case of increase of 50% resistance..... 72
Figure 4.25 Output for the case of increase of 100% resistance..... 72
Figure 4.26 Output for the case of decrease of 5% resistance 73
Figure 4.27 Output for the case of decrease of 10% resistance 74
Figure 4.28 Change of resistance for Wheatstone bridge 76
Figure 4.29 Response of Sensor to the change in resistance of gas sensitive resistor..... 77
Figure 5.1 Layout for first configuration of the gas sensor (layout floorplanning)..... 80
Figure 5.2 Comparison of schematic and post-layout simulation for first configuration. 81

LIST OF ABBREVIATIONS

WSN	:	Wireless Sensor Network
WPAN	:	Wireless personal area network
WLAN	:	Wireless local area network
GSM	:	Global System for Mobile communication
GPRS	:	General Packet Radio Service
CDMA	:	Code division multiple access
RFID	:	Radio-Frequency Identification
mW	:	milliwatt
ADC	:	Analog to digital converter
DAC	:	Digital to Analog Converter
CMOS	:	complementary metal-oxide-semiconductor
LNA	:	Low noise amplifier
GHz	:	Giga Hertz
GPS	:	Global positioning system
PWM	:	Pulse width modulation
AC	:	Alternating Current
DC	:	Direct Current

PMOS	:	P-type Metal Oxide Semiconductor
NMOS	:	N-type Metal Oxide Semiconductor

ABSTRACT

Full Name : [Hamza Shahid]

Thesis Title : Power Efficient Wireless Sensors for Gas Concentration Measurement

Major Field : [Electrical Engineering]

Date of Degree : [April 2017]

Wireless/mobile sensors have newly been considered in monitoring industrial applications including risky gasses location. These types of sensors are of particular importance for the Saudi industry in refineries and petrochemical plants. As a significant energy users, gas sensors might essentially limit their lifetime. Hence, the sensing circuit is carefully designed to optimize power consumption while achieving the desired performance and accuracy. The metal oxide from which these sensors are made of (mostly SnO2-based), has a range of temperature for sensing different gasses. Hence, the same sensor can be used by different applications for measuring different gasses. The ideal temperature for metal oxide (SnO2) to sense CH4 is 400 °C while it is 90 °C for CO.

The main objective of this thesis is to design a low power wireless sensors for gas concentration measurement such that it can be utilized in the harsh environment for a long period of time. Typical wireless sensor has main blocks of sensor front end, micro-heater, microcontroller, power management, memory and communication block. After microheater, the most power hungry component in sensor is microcontroller. The main function of microcontroller is to provide the clock timing for the sensor operation. It is also used for signal conditioning and memory. This work suggests adoption of a sub-hertz oscillator, which has very low power consumption, for providing the timing for sensor instead of the microcontroller. A microcontroller but at the receiver end, where utility power sources are available, can be used to analyze the transmitted signal and add various signal conditioning attributes. Several circuit techniques are utilized to achieve the purpose of gas sensing more efficiently while keeping the sensitivity comparable and reducing power consumption.

The sensor circuit uses two oscillators, a sub-hertz for providing the operating time of sensor while the other for generation of AC signal to excite the Wheatstone bridge based

sensor front end. The sub-hertz timer utilizes sub-threshold operation of transistors to realize a CMOS inverter based Schmitt trigger. The current for charging and discharging of capacitor is reduced in order to obtain ultra-low frequency oscillation. In addition, a novel inverter based Schmitt trigger is proposed which is used to provide the AC signal to sensor front end with improved sensitivity. The sensitivity of the wireless sensor is further improved by using a high gain difference amplifier providing a gain of 63.5 V/V which makes the output range of 1V for full scale variation. This allows to take the measurement at lower temperatures when the resistance starts changing. The average power consumption of the whole circuit is 38.77μW apart from the micro-heater power consumption. It is possible to estimate the overall power consumption of the system by adding the power of a commercial microheater and communication block to be around 2.07mW which is around 40 times less than the available solutions.

The thesis consists of seven chapters. The first chapter include an introduction, motivation, the problem statement, an outline of objectives and the contributions. In chapter # 2, literature review is discussed. A detail discussion on different specifications of wireless gas sensors is presented in this section. In chapter #3, the approach towards achieving the goal will be explained with all the circuits involved and their explanation. The results for each stage as well as the final results are summarized in Chapter #4. Chapter # 5 contains the new proposed Schmitt trigger for timer circuit. Chapter # 6 shows the post layout simulation and Chapter # 7 consists of conclusion and future directions.

ملخص الرسالة

الاسم الكامل: حمزة شاهد

عنوان الرسالة: أجهزة استشعار لاسلكية ذات كفاءة عالية لاستهلاك الطاقة لقياس تركيز الغاز

التخصص: الهندسة الكهربائية

تاريخ الدرجة العلمية: 19-رجب-1438 هجري

تستخدم أجهزة الاستشعار اللاسلكية / المحمولة حديثا في رصد مواقع التطبيقات الصناعية بما في ذلك الغازات الخطرة. هذه الأنواع من أجهزة الاستشعار ذات أهمية خاصة للصناعة السعودية في معامل التكرير والبتروكيماويات. لكن بسبب استهلاكها لطاقة كبيرة، تحد أساسا من حياتهم التشغيلية. وبالتالي، من المهم تصميم دائرة الاستشعار بعناية لتحسين استهلاك الطاقة مع تحقيق الأداء المطلوب والدقة. وتصنع هذه الأجهزة الاستشعارية من أكسيد المعادن (معظمها على أساس SNO2)، وتتمتع بأن لديها مجموعة من درجة الحرارة لاستشعار الغازات المختلفة. وبالتالي، يمكن استخدام نفس أجهزة الاستشعار من قبل تطبيقات مختلفة لقياس الغازات المختلفة. فمثلاً درجة الحرارة المثالية لأكسيد المعادن لاستشعار الميثان هي 400 درجة مئوية بينما هو 90 درجة مئوية لأول أكسيد الكربون.

الهدف الرئيسي من هذه الرسالة هو تصميم أجهزة استشعار لاسلكية منخفضة الطاقة لقياس تركيز الغاز بحيث يمكن استخدامها في بيئة قاسية لفترة طويلة من الزمن. ويحتوي التكوين النموذجي لجهاز الاستشعار لاسلكي على كتل رئيسية من أجهزة الاستشعار الأمامية، سخان صغير (ميكروهيتر)، متحكم، إدارة الطاقة والذاكرة، وكتلة الاتصالات. ويستهلك المتحكم معظم طاقة أجهزة الاستشعار وذلك بعد الميكروهيتر. وتتمثل المهمة الرئيسية للمتحكم في توفير توقيت لعملية الاستشعار على مدار الساعة. كما أنه يستخدم لتحليل الإشارات والذاكرة. ويقترح هذا العمل استخدام مولد ذبذبات ذا تردد تحت واحد هيرتز، والذي يتميز باستهلاك طاقة منخفضة جداً، لتوفير التوقيت لجهاز الاستشعار بدلا من المتحكم. ويمكن استخدام متحكم ولكن في جهاز الاستقبال، حيث تتوفر مصادر طاقة من المرافق، لتحليل الإشارة المرسلة وإضافة سمات تكييف الإشارات المختلفة. ولقد تم استخدام العديد من تقنيات الدوائر لتحقيق الغرض من استشعار الغاز بشكل أكثر كفاءة مع الحفاظ على حساسية مقبولة والتقليل من استهلاك الطاقة.

وتستخدم دائرة الاستشعار المقترحة اثنين من مولدات التذبذب، احدهما مولد الذبذبات ذا تردد بمقدار مليهيرتز لتوفير وقت التشغيل لجهاز الاستشعار والأخر لتوليد إشارة مترددة لإثارة جسر ويتستون في الجبهة الأمامية للمستشعر. وتم تصميم مولد الذبذبات ذا تردد مليهيرتز باستخدام الترانزستورات تعمل تحت فاصل التشغيل موصلة على شكل زناد-شميت العاكس.حيث يتم شحن وتفريغ مكثف بصورة خاصة من أجل الحصول على التردد متناهي الانخفاض.بالإضافة الى ذلك تم اقترح زناد-شميت عاكس جديد لاستخدامه لتوليد إشارة مترددة الواجهة الأمامية للمستشعر والذي يتمتع بحساسية محسنة. وتم تحسين حساسية جهاز الاستشعار لاسلكي أيضا باستخدام مكبر للفرق والذي يوفر مكاسب بمقدار 63.5 مرة مما يجعل نطاق الإخراج يصل الى V1 للتغير الكامل لنطاق المقاومة المتغيرة. وهذا يسمح لأخذ القياس في درجات حرارة أقل عندما تبدأ المقاومة تغيير. ويبلغ متوسط استهلاك الطاقة من الدائرة بأكملها 38.77 ميكرووات من غير حساب استهلاك طاقة السخان الصغير. ويمكن تقدير إجمالي

استهلاك الطاقة بإضافة ميكروهيتر التجارية كتلة الاتصالات ليصل الى 2.072 ميكروواوات وهو حوالي 40 مرات أقل من الحلول المتاحة.

وتتكون الأطروحة من سبعة فصول. ويتضمن الفصل الأول مقدمة، والدوافع، وبيان المشكلة، وموجزا للأهداف والمساهمات. وفي الفصل 2، يتم مناقشة المراجع العلمية ذات العلاقة مع مناقشة تفصيلية بشأن المواصفات المختلفة لأجهزة استشعار الغاز اللاسلكية. كما يقدم الفصل 3 شرح النهج نحو تحقيق الاهداف مع شرح جميع الدوائر المعنية. ويتم تقديم نتائج كل مرحلة وكذلك النتائج النهائية في الفصل رقم 4. ويحتوي الفصل رقم 5 زناد-شميت الجديد لدائرة الموقت. وفي الفصل رقم 6 يقدم نتائج المحاكاة بع التخطيط. وفي الفصل 7 والاخير يتم عرض الاستنتاجات والاتجاهات المستقبلية.

CHAPTER 1

INTRODUCTION

A sensor is a device that can generate a useable electric signal from a measured physical parameter of the environment. It provides the output as a function of changing the quantity which is to be measured as an electrical signal, optical or electromagnetic signal. It can measure the mechanical, calorific, chemical parameters just like, flow, speed, distance, temperature, force, pressure, concentration, acceleration and composition of gases. For example, a thermocouple senses the temperature and provides the output in the form of electric signal while a mercury in glass based thermometer also senses temperature variation and gives the output as expansion of mercury in the glass which can be seen and measured.

In its simplest form, a sensor consists merely of a naked sensor element, for instance an unhoused pressure sensor element made of silicon, mounted on a substrate, no more than a few millimeters exterior dimension. The term “measuring principle” (also referred to as the “active principle”) is understood to mean the principle of physical or chemical conversion resulting in a usable electrical signal. A measuring parameter is converted into an internal signal by means of the physical measuring principle of the sensor element. After possible signal conditioning, a measured value is available at the output as a usable or electrical signal – for example, luminous intensity as an analogue voltage. The basic scheme is shown by Fig.1.1 [1]

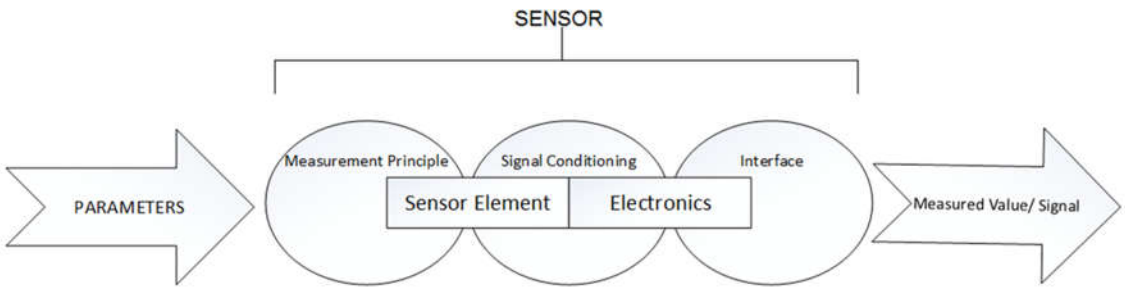

Figure 1.1 Basic elements inside a general Sensor

Sensors are connected to the system via wire or wireless. Wireless sensors are more suitable as they are cost effective, small, and easy to integrate than a typical wired sensor. Wireless sensor are a medium applicable to observe a vast variety of environment parameters, for example acceleration, temperature, pressure and also utilized for war zone observation, environment observing, home automation applications and bio medical applications. Due to the advancement of efficient sensor systems, WSN can be sent in applied in various remote places and cruel climate conditions.

Different Sensing technology are extensively monitored and used for the sensing of the gas detection. As there are various limitations of these gas detection technologies, there are vast area of research for different methodologies for the researchers to work on and acquire the solutions with improved calibration for gas sensors. These wireless sensors for gas monitoring systems can be majorly classified according to change in electrical properties of the material for sensing like [2]

- Metal Oxide Semiconductors (MOS)
- Carbon Nanotubes
- Polymers

- Moisture absorbing materials.

Different methods are utilized to acquire the results which are based on these types of variations like [2]

- Optical
- Acoustic
- Calorimetric
- Gas-chromatography

In this thesis, the emphasis is based on the metal oxide semiconductor based wireless gas sensors. A typical semiconductor based gas sensor is based on micro heater in a Wheatstone bridge or in differential configuration. The micro heater heats the two special resistors in the Wheatstone bridge or the differential configuration. The catalyst is applied over the surface of one of the two sensors which burns in the presence of a gas over the surface of the resistor and the resistance of that resistor with catalyst on the surface changes while the other one remains the same. This provides the change of voltage at the output which is detected by the micro-controller which compares this output voltage from the bridge with the nominal value of no gas situation. If the output voltage is different, the micro controller sends the interrupt signal to the receiver. The receiver then send the signal to the valves to close to avoid any hazard.

1.1 Motivation

Wireless devices are one of the technologies on which large improvements are emerging from past years. The range of these devices covers from basic IrDa which is based upon infrared region for a short distances communication between a sender and a receiver to WPAN for short distance but multiple receivers, to medium range communication in WLAN, to far distance communication networks like GSM, GPRS and CDMA. [3]

The capacity to identify the events happened, is vital to the achievement of developing wireless sensor technology. Wireless/mobile sensors offer an effective blend of the power of sensing, manipulating and communicating with other devices. They are being used in vast range of applications and, in the meantime, offer various trials because of their characteristics, essentially the severe energy requirements which these sensors usually face. The reduction in need of wiring and simplification of the circuit is a benefit of mobile sensors. The experimentation stage in hardware platforms are been planned for the testing of new incoming ideas given by the research community and how to implement those design in the real world to get the desired outputs.

Mobile sensors bring the applications which were impossible without it, for example, observing hazardous, dangerous, unwired or remote ranges and areas. The mobile sensors give about huge installation adaptability to sensors and enhanced the efficiency of the system. Besides mobile sensors lower the maintenance skills of the system and reduces the expenses. Mobile sensors and sensor systems are widely used in farming and nourishment generation for ecological observing, agriculture [4], food, monitoring of environment [5-6], modern vehicles, building and office mechanization and RFID-based tracing frameworks. [7]

1.2 Requirements from a sensor

A sensor should respond to the requirements for which it is designed. A sensor should have following characteristics [2]

- **Uncertainty:** Attainment of minimal measuring uncertainty.
- **Availability of Data:** Constant availability of physical and chemical data from all systems and processes
- **Impact:** Measurements are to be performed with minimal impact on the processes involved
- **Real Time:** Measuring values are to be available in real time
- **Interference:** Sensor should work with minimal interference and a minimum of care
- **Cost:** Sensor and sensor-system costs should be as low as possible
- **On Board Diagnostic**: Sensors are to be equipped with integrated "on-board" diagnostic
- **Ruggedness:** It should be able to withstand the overload with the help of protection provided.
- **Linearity:** The sensor should have the linear input and output characteristics.
- **Repeatability:** The sensor should give the same output when the similar input is given to the sensor.
- **Quality:** The sensor should give the high-quality output signal.
- **Reliability:** The sensor should be reliable and stable. Sensors should function without maintenance, calibration, or adjustment.

- **Dynamic Response:** The sensor should have a vast dynamic response.
- **Hysteresis:** The sensor should not show hysteresis

1.3 Thesis Objectives

The main objective of this work is to propose circuit techniques for designing a wireless gas sensor with improved power consumption and hence increased the lifespan of the sensor. This is accomplished by modifying the sensor front end to achieve the measurement with desired sensitivity but with less power consumption. This allows taking the measurement at lower temperatures when the burning of a specific gas starts. Also, the proposed work applies the heating profile efficiently to get the desired results while minimizing the power consumption. The results of the sensors can be applied to industries containing hazardous gas (like petroleum and gas industry, chemical industries etc.) as well as for environment monitoring in the industrial areas.

1.4 Thesis Methodology

The thesis work is divided into following tasks:

Task 1: Available solutions assessment and literature survey

- Explore different industrial gas monitoring sensors and evaluate the performance of these gas sensors.
- Surveying application of different techniques to design a gas monitoring sensors.

Task 2: Design of sensor front end

- Evaluating the two different approaches of Wheatstone bridge and differential configuration for the sensor front end based on sensitivity and performance.

Task 3: Heating profile for the sensor

- Analyzing heating profile to be applied to the micro heater to heat the sensor to the required temperature efficiently.

Task 4: Assessing the approaches for output measurement

- The different techniques will be assessed for measuring the change of resistance from the sensor front end.

Task 5: Designing and simulation

- The circuit design and simulations will be carried out in Cadence® and the output results will be shown.

1.5 Thesis Contribution:

Gas sensors from the last decade is a very popular topic of research in academia and industry due to the enhancement required for these kinds of sensors with the passage of time. Wireless Gas sensors are beneficial over the wired sensors because of the harsh environment in which the sensors have to work, cost of cables is reduced, and lower maintenance is required as well as the fault can be easily detected. The major problem with the wireless gas sensors are the huge power consumption, due to heating in CMOS and other processes in different types of wireless gas sensors. Large power consumption requires large supply power which is usually provided by batteries in the wireless sensors.

The batteries supply this power for the limited amount of time and there is need of replacement of these batteries after a short time interval which creates a problem as these sensors are usually located at unreachable places or in harsh environments, so the lifetime of theses sensors is a major issue in the usage of theses sensors. Due to the high-power consumption, energy harvesting techniques cannot provide the energy in milliwatt (mW) range in indoor environment [8].

This thesis will contribute in the design of smart gas sensors for industrial monitoring for which will be useful for the oil, gas, paint and other chemical industries in the kingdom of Saudi Arabia as well as other countries.

1.6 Thesis Breakdown

The thesis consists of seven chapters. The first chapter include an introduction, motivation, the problem statement, an outline of objectives and the contributions. In chapter # 2, literature review is discussed. A detail discussion on different specifications of wireless gas sensors is presented in this section. In chapter #3, the approach towards achieving the goal will be explained with all the circuits involved and their explanation. The results for each stage as well as the final results are summarized in Chapter #4. Chapter # 5 contains the new proposed Schmitt trigger for timer circuit. Chapter # 6 shows the post layout simulation and Chapter # 7 consists of conclusion and future directions

CHAPTER 2

LITERATURE REVIEW

This section discusses different approaches for wireless sensors applied in industry and academia from past decade and summarize the different methods applicable to achieve the function of gas monitoring by different techniques.

2.1 Background:

From the last decade, the sensing of the gas is one of the major application of industrial safety and monitoring. The research is going on in academia as well as in industry for making the sensors better and more energy efficient with every passing day. The common areas Gas sensing technology has become more significant because of its widespread and common applications in the following areas: (1) industrial production (e.g., methane detection in mines) [9-10] ; (2) automotive industry (e.g., detection of polluting gases from vehicles) [11] ; (3) medical applications (e.g., electronic noses simulating the human olfactory system) [12] ; (4) indoor air quality supervision (e.g., detection of carbon monoxide) [13] ; (5) environmental studies (e.g., greenhouse gas monitoring)

During the last fifty years, different studies have established various branches of gas sensing technology. Among them, the three major areas that receive the most attention are investigation of different kinds of sensors, research about sensing principles, and fabrication techniques [14-15]. In these papers, a classification of sensing technologies is given, followed by descriptions of the main technologies to provide a comprehensive review. Two key performance indicators are highlighted, to introduce and compare

different sensing technologies. Current research status and recent developments in the gas sensing field are reported, to discuss potential future interests and topics. Moreover, suggestions on related topics' future development are also proposed

2.2 Applications of Wireless Sensors:

The general applications of Wireless sensors cover every field of science and technology, from basic household items to complex systems of industries. Figure 2.1 shows the general applications of wireless sensors. The basic areas are shown which can have the use of wireless sensors in more than one applications in the respective area [9-19].

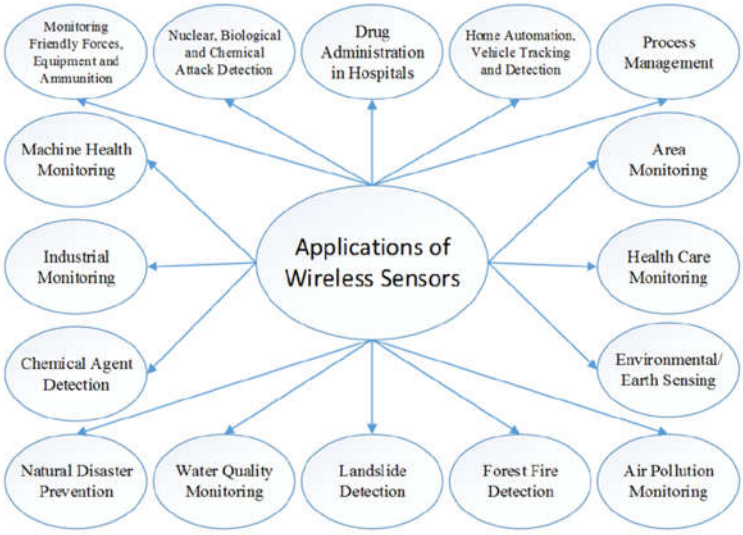

Figure 2.1 General Applications of Wireless Sensors

Gas sensing by the help of mobile sensor is becoming mere significant due to the utilization of such sensors in the areas of (1) industrial production which includes the detection of methane gas in the mines [9], (2) in the automotive industries which includes the detection of gasses causing pollution coming out from the vehicles [11], (3) in the field of medical regarding the detection of hazardous gases for human respiratory system [12], (4) the

monitoring of air quality inside a building which includes the detection of carbon monoxide and carbon dioxide etc. (5) To study the environmental effects of different gases e.g. in the monitoring of greenhouse gases [13]. Details of these areas will be mentioned in the of literature review.

2.3 Classification of Gas sensors based upon method of sensing

The sensing of the gas basically is divided in two basic modules which can be further divided into separate sections. The two basic methods include the variation in the electrical properties of the gas sensor and the other properties of the sensors. The classification of these sensors in shown in Figure 2.2 [2].

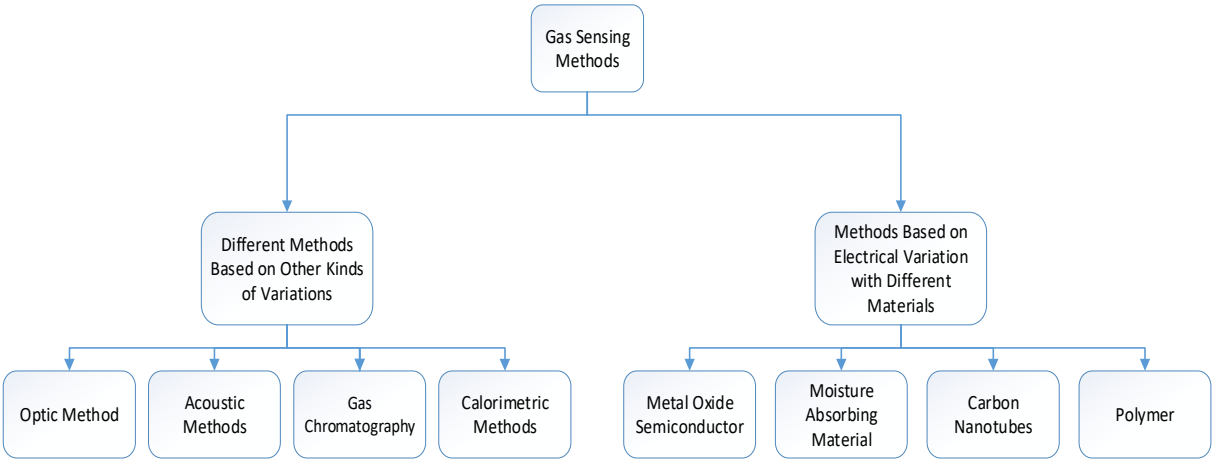

Figure 2.2 Classification of Gas Sensing Methods

2.4 Evaluation of Gas Sensing Methods:

The evaluation of theses gas sensing methods is based on different parameters which should be considered for the selection of a certain method from the others. (1) The sensitivity of the sensor, which includes the threshold value for the target gas as well as the minimum concentration of that gas to be measured. (2) The selectivity of the sensor, which

make sure to detect a certain gas when the combination of different gases are present. (3) The response time of the sensor which includes the time between the concentration of the gas to the certain value and when the sensor detects that and responds. (4) The energy or power consumption of the specific sensor. (5) The reversibility of the sensor to its original state after the measurement of a certain gas. (6) The absorbent ability of the sensor that it can absorb the moisture and the reading is not affected by the moisture. (7) The cost of fabrication for the sensor which can vary for the different methods and the usage of that sensor in a particular environment. [14]

Although the sensors are designed to give the desired results for a long period of time and their efficiency should remain the same but the performance of these sensors may degrade with one of these reasons which can cause the major fail in the safety requirements of a certain setup and a loss of human life and property may occur. (1) The design error in the sensor which can be avoided by the careful inspection of the sensor in the test phase before the commercial production. (2) The change or variation in the structure of the sensor when the measurement is taken from it. (3) The lag or phase shift in the reading of the sensor due to some additional doping on the sensing layer of the sensor. (4) The change in the chemical properties of the sensor due to the chemical reaction of certain gas on the sensor. (5) The effect of environmental factors which can alter the response of the sensor for a specific gas. Table 2.1 shows the advantages, disadvantages and applications of these sensors. Usually the gas sensors mostly used were based on film based, optical based or the semiconductor and catalytic based. Film based sensors uses the combination of a colorimetric chemical sensor along with the sensor for intensity of light [20]. The sensor receives the intensity of light which is changed by the presence of hazardous gas in the form of change in color of

the film. These kinds of sensor although have very low power consumption but large response time which makes them unsuitable for deployment by taking care of safety requirements. Optical based sensors are employed with the help of laser-spectroscopic trace gas sensors [20]. These sensors detect the little traces of gas concentration based on calculation of ppm or ppb (parts per million or parts per billion). Although these sensors are very accurate and response time is very less according to the safety requirements but the power consumption of theses sensors is very high and draws a huge amount of current (around 500mA) which makes them imperfect for wireless based sensors. The catalytic or semiconductor based sensor are in between the two of them having the less power consumption than the optical based sensors and are fast and selectable as compared to film based sensors [2].

Table 2.1 Advantages, disadvantages and applications of different Gas sensors

Materials	Advantages	Disadvantages	Target Gases and Application Fields
Metal Oxide Semiconductor	(a) Low cost; (b) Short response time; (c) Wide range of target gases; (d) Long lifetime.	(a) Relatively low sensitivity and selectivity; (b) Sensitive to environmental factors; (c) High energy consumption.	Industrial applications and civil use.
Polymer	(a) High sensitivity; (b) Short response time; (c) Low cost of fabrication; (d) Simple and portable structure; (e) Low energy consumption.	(a) Long-time instability; (b) Irreversibility; (c) Poor selectivity;	(a) Indoor air monitoring; (b) Storage place of synthetic products as paints, wax or fuels; (c) Workplaces like chemical industries.
Carbon Nanotubes	(a) Ultra-sensitive; (b) Great adsorptive capacity; (c) Large surface-area-to-volume ratio; (d) Quick response time; (e) Low weight.	(a) Difficulties in fabrication and repeatability; (b) High cost.	Detection of partial discharge (PD)
Moisture Absorbing Material	(a) Low cost; (b) Low weight; (c) High selectivity to water vapor.	(a) Vulnerable to friction; (b) Potential irreversibility in high humidity.	Humidity monitoring
Optical Methods	(a) High sensitivity, selectivity and stability; (b) Long lifetime; (c) Insensitive to environment change.	(a) Difficulty in miniaturization; (b) High cost.	(a) Remote air quality monitoring; (b) Gas leak detection systems with high accuracy and safety; (c) High-end market applications.
Calorimetric Methods	(a) Stable at ambient temperature; (b) Low cost; (c) Adequate sensitivity for industrial detection (ppth range).	(a) Risk of catalyst poisoning and explosion; (b) Intrinsic deficiencies in selectivity.	(a) Most combustible gases under industrial environment (b) Petrochemical plants; (c) Mine tunnels; (d) Kitchens.
Gas Chromatograph	(a) Excellent separation performance; (b) High sensitivity and selectivity.	(a) High cost; (b) Difficulty in miniaturization for portable applications.	Typical laboratory analysis.
Acoustic Methods	(a) Long lifetime; (b) Avoiding secondary pollution.	(a) Low sensitivity; (b) Sensitive to environmental change.	Components of Wireless Sensor Networks.

So our prime interest will be on metal oxide semiconductor based wireless sensors for compact low power sensors with acceptable sensitivity.

2.5 Approaches for Metal Oxides semiconductor based Gas Sensors:

The popular approaches for wireless gas sensors are described in Figure 2.3. Every approach has its own advantages and disadvantages and one must critically analyze each

of them to be suitable for their target application. These approaches are analyzed and most suitable configuration is used which is described in detail in the next chapter.

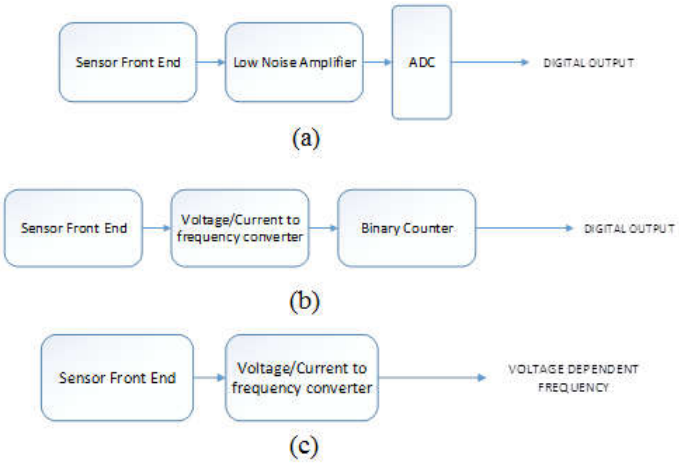

Figure 2.3 Approaches for Wireless Gas Sensors

The approach in (a) converts the front-end voltage /current to digital by the help of low noise amplifier (OP amp based) and then ADC to convert the amplified signal into digital [21]. The approach (b) converts the sensor front end voltage/current into frequency dependent of incoming voltage /current and then a binary counter is utilized to convert that frequency into digital output [22]. The approach (c) is utilized when the output required is a voltage dependent frequency and that change in frequency determines the presence of a specific gas [22].

2.6 Blocks of Wireless Gas Sensors:

Typically, the Wireless sensors has the followings blocks which will be described in a brief detail in order to understand the purpose of each block.

2.6.1 Sensor Front End:

The sensor front end circuit is usually based on the Wheatstone bridge circuit, which comprises of two sensing resistors and two normal resistors to complete the bridge circuit. The power is generally consumed in the sensing resistors as compared to the other resistors when the measurement is taken. CMOS based micro heaters are utilized to heat up the resistances up to the required temperature with low power consumption and higher efficiency [14]. One of the two sensing resistors is gas sensitive resistor due to the catalyst. The catalyst is applied over the main measurement resistor and the reference sensing resistors does not have catalyst on its surface. The oxidation of the gas starts at around 200 ^{o}C and the gas starts burning over the surface of the resistor. The change in resistance of the sensing resistor with catalyst on the surface starts from this temperature but the change is too small. It begins to increase with the increase of temperature. When the resistors are heated to almost 400^{o}C, the catalyst burns over the surface of main sensing resistor and its resistance changes fully while the resistance of other sensing resistor without the catalyst remains the same. The different output is obtained then the situation when gas is not present. When gas is not present, the catalyst doesn't burn and resistance of both sensing resistances remains the same giving the zero output although if there is some change in resistance due to high temperature, it is minimized due to the cancelling structure of wheatstone bridge as it will come in both sensing resistors and will affect them equally which will neglect the effect.

Due to the two-sensing resistor, the Wheatstone bridge configuration consumes more power, the sensing front end sensor can also be based on voltage divider circuit which is termed as differential circuit in [8] although it does not provide the differential output and

name is adopted as the output voltage changes with respect to the change in resistance and then the difference is taken from the original value. Many articles in literature claims to achieve low power consumption as there is only one sensing resistor and one reference resistor as compared to the Wheatstone bridge which has two of both. The only difference comes in the sensitivity of the sensor front end which is significantly reduced in the differential based circuits as compared to wheatstone bridge. The circuit schematic of both the approaches are shown in Fig 2.4 [8].

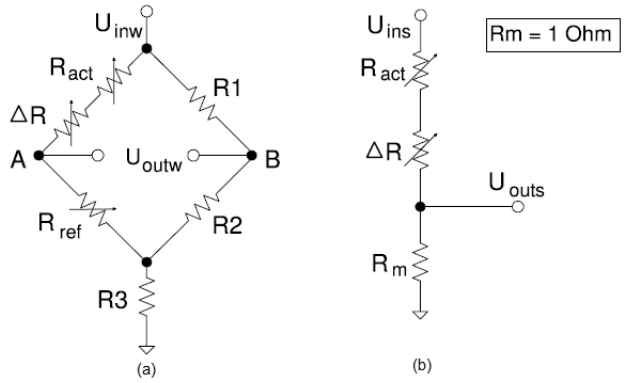

Figure 2.4 Sensing front end circuits (a) Wheatstone (b) Voltage Divider

2.6.2 Drawback of the approach:

The circuit suggested in (b) comes with only one sensing resistor and consumes less power, but the issue of environmental factors is still there and the circuit is not much efficient. If the resistance of the sensing resistor changes just due to very high temperature, it will give the different output which can trigger the false alarm. The wheatstone bridge on the other hand has four resistors with two sensing resistors and two reference resistors, the power consumption is more. So we had to come up with the solution to resolve both the problems while keeping the sensitivity as high as possible.

2.6.3 Low Noise Amplifier:

A low-noise amplifier (LNA) is an electronic amplifier that amplifies a very low-power signal without significantly degrading its signal-to-noise ratio. An amplifier increases the power of both the signal and the noise present at its input. LNAs are designed to minimize additional noise. Designers minimize noise by considering trade-offs that include impedance matching, choosing the amplifier technology (such as low-noise components) and selecting low-noise biasing conditions.

LNAs are found in radio communications systems, medical instruments and electronic equipment. A typical LNA may supply a power gain of 100 (20 decibels (dB)) while decreasing the signal-to-noise ratio by less than a factor of two (a 3-dB noise figure (NF)). Although LNAs are primarily concerned with weak signals that are just above the noise floor, they must also consider the presence of larger signals that cause intermodulation distortion.

The second stage in the sensor will be based on LNA (low noise amplifier). LNA should be broadband to have a reliable matching of the input, more linearity, and the noise figure should be low over a wide bandwidth of GHz, but having very little power consumption and very small area to be easily fitted on a chip. The major challenge for the design of ultra-wide band LNA is the linearity which should be high through all of the available bandwidth. The optimization of the overdrive voltage is one of the methods to improve linearity for the small input amplitudes and it will increase the response to the process variation. It is usually effected by the low supply voltage and the mobility effects of high fields [23]. The output from the first stage of sensor front end in the form of voltage or current is then sent to a LNA. The measurement from the sensor front end has a very small

difference when the gas is present and when gas is not present. The low noise amplifier voltage or current mode with a proper gain can be utilized at this stage to get the required outputs.

The (MAX2659) low-noise amplifier has a large gain which is designed to be used portable and handheld devices like GPS, GLONASS and Galileo. The amplifier is very ideal to be used for a global positioning system to be added to a small navigational device as well as cell phones to use this feature for personal mobility.

Although the MAX2659 has sufficient linearity for most of the system applications but still we can improve the IP3 of the device. This is achieved by using a degeneration inductor among the port number 2 which is the emitter of the amplifier and ground terminal, which is described in Figure 2.5. This would increase significantly the IP3 meanwhile this will reduce the gain of the amplifier along with the little degradation of the noise figure.

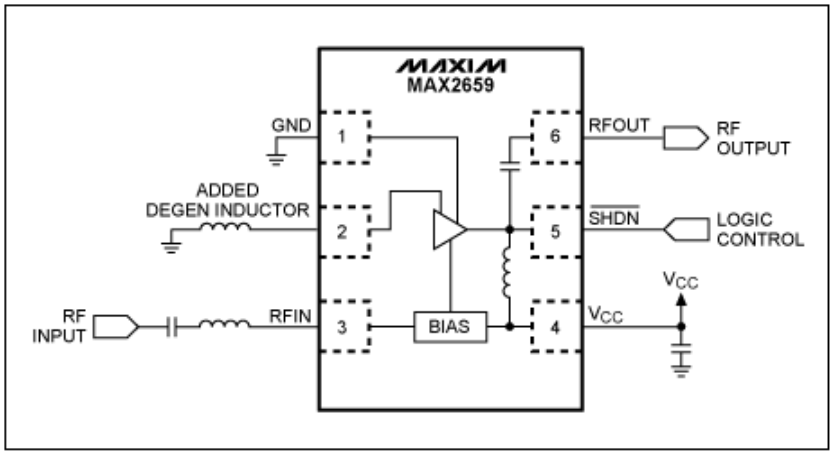

Figure 2.5 Typical application circuit for increased linearity.

The problem with these LNA is the huge power consumption in mW range, which makes them difficult to use in low power solutions. The second thing is the use of inductors in the circuit design which will make the integration difficult and CMOS realization of these

inductors will add power consumption of the circuit. Even a low voltage LNA having supply voltage of 0.4V is having the power consumption of 1.03mW [24]. The microcontroller can read the signal directly from sensor front end without the need of amplification on the cost of such power. So, the LNA stage can be avoided in the design according to the requirement of specific application of these wireless gas sensors.

2.6.4 Microcontroller:

The major block of these wireless gas sensor is the microcontroller unit which performs all the required tasks for the wireless gas sensor. It works as a main control unit for all the activities that are performing inside the sensor circuit. The micro controller is power hungry element after the micro-heater in the gas sensor. The power in the range of mW is required to carry out all the functions. These microcontrollers are very popular with the gas sensors as they provide a wide range of possibilities which can be easily achieved with the presence of microcontrollers with a little sacrifice of power consumption. So different techniques such as pulse width modulation (PWM), on- off timing, heating profile, sleep mode are used in order to save the power when using the microcontroller in the sensor node.

The microcontroller consists of the blocks like programmable memory, comparators, oscillators, ADC, DAC, timers/ counters, reset and power on circuits and they are also used to control the other blocks like transmitters, receivers, supply control circuit etc. Typically, these are targeted for the applications like

- Industrial control
- Climate control

- Hand-held battery applications
- Factory automation
- ZigBee
- Power tools
- Building control
- Motor control
- HVAC
- Networking
- Optical
- Medical Applications

Different microcontrollers are used in literature in order to achieve the desired result with minimum power consumption. Atmel ATxmega32A4 is preferred in most of the sensors due to small sleep current of 1 μA and 12bit ADC and DAC. During the operations, its current is in mA as it controls all the function which includes the circuit management, the heating profile of the sensor as well as communication with transmitter module. [25]

Following blocks of microcontroller are often used in the gas sensors for performing the proper operation of the sensing.

2.6.3.1 Analog to Digital Converter (ADC)

One of the important block in a microcontroller is the availability of analog to digital converter. The ADC will be required to convert the analog form of voltage or current to digital form which can be easily transmitted to the receiver end. The resolution and power consumption of ADC are important factors which must be considered according to the

required situation. The available types of ADC which includes SAR, Delta-Sigma and Pipeline gives the range of resolution on the expense of power consumption. The SAR ADC with maximum of 16 is usually utilized when it is used separately with minimum power consumption of the three types. The microcontroller mostly used in gas sensors have 12-bit ADC in them like in ATxmega32A4 The typical power consumption of SAR ADC for 9 bits of resolution is described as 1.2µW with max frequency of 1.1MHz in [26]. The optimum condition is achieved with lower power of sensor front-end and a little more power of ADC for better resolution at lower temperature will be followed in order to get the acceptable results with overall low power consumption of the sensor. The low power ADC proposed in [26] is shown in Figure 2.6.

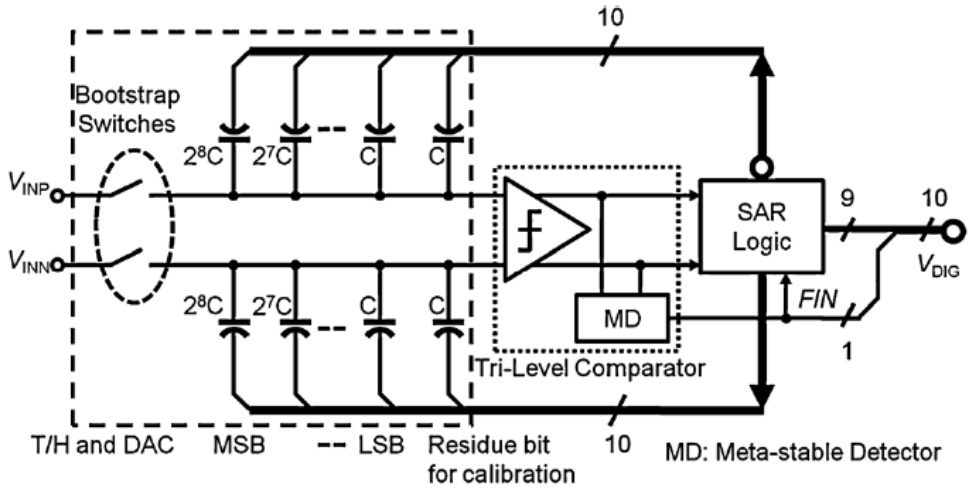

Figure 2.6 Tri-level comparator SAR ADC architecture

The timing for the comparator is relaxed and the resolution of the ADC is reduced to one bit by reducing the power consumption very low and very low supply voltage is required. As for the gas monitoring sensor, very high frequency is not required and the process of measurement only takes place once or twice in a minute so we can tradeoff the speed of conversion and reduce the power consumption of the block.

2.6.3.1 Binary Counter:

Usually a 32-bit counter is available in the microcontroller that can even run during the sleep mode in order to carry out the tasks such as heating of the sensor front end after a specific amount of time. The counter/timers are really important for the microcontroller to perform the required tasks. With the help of these counter, the sub hertz frequency is achieved with the help of programming to turn on the heater after the specific amount of time.

In the approach consisting of voltage/current to frequency converter. asynchronous counters are usually utilized to convert the frequency generated in the voltage/current to frequency converter block to digital values. The block diagram for the binary counter is given in Fig. 2.7 [27].

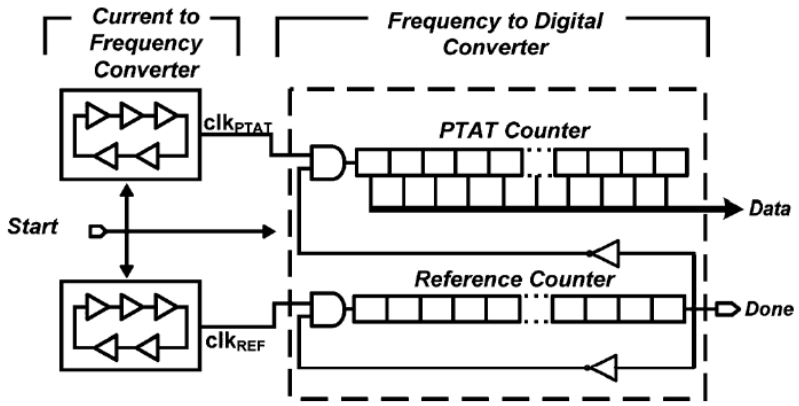

Figure 2.7 Block diagram of frequency to digital converter

The counter is selected up to 9-bit resolution and the reference counter is also there to compare the results for the reference frequency and the frequency we are getting from previous stage. The comparison of the two is obtained the results are sent to next stage for transmission to receiver end.

2.6.3.3 Sensor Heating Profile:

To save the power consumption of the wireless sensor, the sensors are not continuously heated, instead they are heated after a regular interval as well as in different manners to reduce the power consumption and get the required results. This is achieved by the programming of microcontroller. The timer in the microcontroller runs even in sleep mode to count the required time after which one level of voltage is applied to the sensor front end and after required time, another value of voltage can be applied. This follows according to the desired pattern fed through programming in the microcontroller. Some of the traditional heating profiles are shown in Figure 2.8.

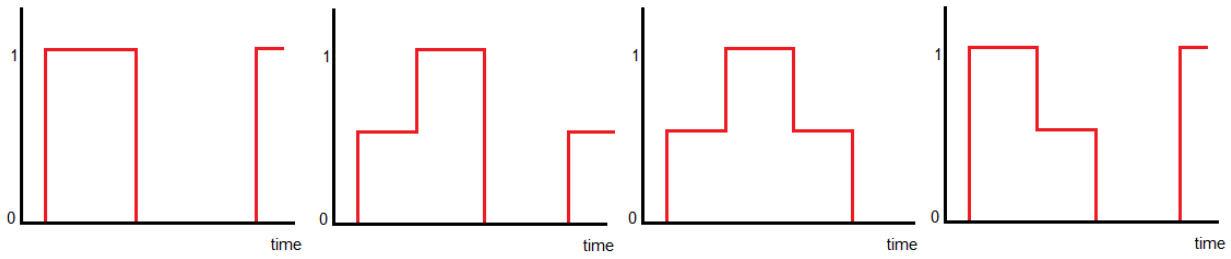

Figure 2.8 Sensor heating profiles with time

As the microcontroller is not used so the heating profile will be first one with two voltage levels high and low produced by sub hertz timer.

2.6.5 Voltage/Current to frequency Converter:

The other approach from low noise amplifier and ADC is to use the voltage to frequency conversion. The output voltage/current from the sensor front end is fed to the voltage controlled ring oscillator which is composed of inverter which is followed by a TG (transmission gate). The NAND gate is used to minimize the static power consumption in idle state which prevents the needless oscillations. The frequency of oscillations is determined by the change of resistance of the TG with the V_H and V_L from the sensor front

end stage. The output power is termed as 71 nW which is very suitable to be used in wireless sensors for low power applications. [22]. The circuit schematic is shown in Figure 2.9

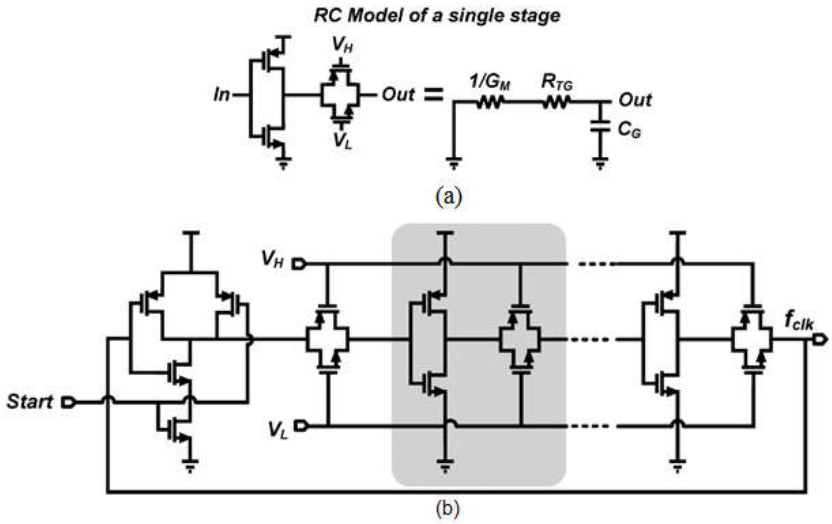

Figure 2.9 Circuit diagram of a voltage controlled ring oscillator.[3]

Another approach uses Buffered source-coupled Multi-vibrator circuit to generate the frequency proportional to the change of output from the sensor front end. The low power consumption of theses sensors is around 600nW with 0.9V supply. The circuit is capable of providing waveforms with symmetry and also high frequency of oscillations. The circuit schematic is shown in Fig 2.10 [27].

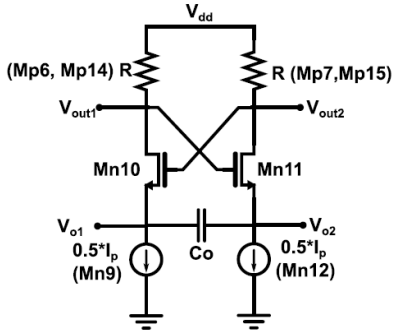

Figure 2.10 Schematic circuit for source coupled multi-vibrator

The cross coupled NMOS transistors will provide a gain stage that drives the load resistance R. The switching in alternate cycles for the cross coupled transistors charges and discharges the floated capacitor C_o. The frequency of oscillations will be directly depending upon the output voltage and input current and the value of capacitor [4].

$$f_0 = \frac{I_p}{4C_0V_0} \tag{2.1}$$

2.7 Benchmark table:

Table 2.2 shows some research work purely regarding the gas sensors and their power consumption. [8]

Table 2.2 Power Consumption comparison for different sensor circuits

	Ho [26]	Wobscholl [27]	FlyPort [28]	Somov 2011 [29]	Yokosawa [30]	Somov 2012 [31]	Somov 2014 [1]
Year	2007	2006	2013	2011	2008	2012	2014
Application	Hazardous gases detection	Toxic gases monitoring	LPG, natural/town gas	Combustible gases monitoring	Hydrogen monitoring	Hazardous gases monitoring	Hazardous gases monitoring
Sensing power consumption	1550 mW	1000 mW	800 mW	264 mW	200 mW	124.30 mW	85.68 mW
Response time	N/A	up to 110 s	up to 10 s	1.50 s	up to 1.20 s	0.70 s (2 sensors) 0.56 s (1 sensor)	0.65 s (2 sensors) 0.50 s (1 sensor)
Sensor	Laser spectroscopic	Catalytic/ semiconductor	Semiconductor	Semiconductor	FET	Catalytic	Catalytic
Features	Detects any gases, accurate measurements, high power consumption	Automatic calibration	Inaccurate measurements, frequent calibration required	Wheatstone circ., accurate measurements	Long sensor response	Differential circuit, accurate measurements, no calibration required	Differential circuit, accurate measurements, no calibration required

The trend of power consumption is given in mW for the references and still it is not a low power circuit which can be operated totally on energy harvesting. The response time is acceptable if it is less than a minute to avoid any loss of life and assets in the emergency condition. By means of differential mentioned in the table, the author means the voltage divider circuit.

CHAPTER 3

GAS SENSOR: INTEGRATED CIRCUIT APPROACH

This chapter begins with major idea of the proposed integrated approach towards the design of wireless gas sensor. Instead of microcontroller, a sub hertz oscillator is proposed to provide the on off timing for the sensor which is the prime objective of the microcontroller. The secondary functions of microcontroller which contains the memory and signal conditioning circuit is taken at receiver end and performed there to save the power. The flow diagram for the proposed sensor approach is shown in figure below.

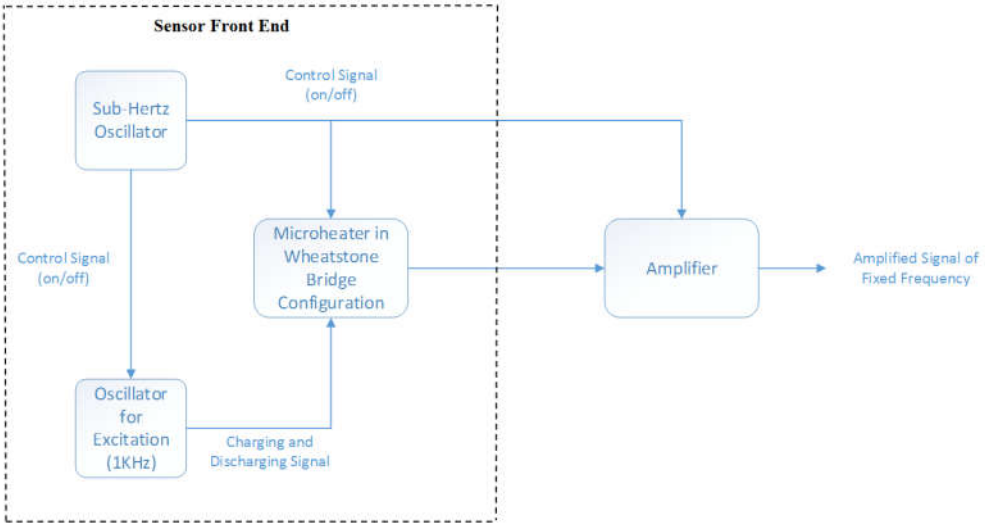

Figure 3.1 Flow diagram for the proposed sensor approach

The simulation is carried out in Cadence® with 0.15um CMOS technology and results will be displayed. The main target of this approach is to reduce the overall power consumption of the wireless sensor by keeping the sensitivity of the sensor as priority. Different energy saving techniques as well as the steps to make the gas sensor smart are discussed in this

chapter with details. The multistage configuration is also demonstrated for larger DC output voltage

3.1 Sub hertz Oscillator

The very first stage for the wireless gas sensor would be its timed on-off switching in order to save power while maintaining the required time of operation. The micro-heater should be heated in a pulsating manner instead of continuous manner which is the major cause of power consumption in a wireless gas sensor. First challenge was to develop the timer/ oscillator which would provide that on-off timing to the sensor front end.

The oscillator required for this purpose was a square wave oscillator which have a logic high and logic low to the switch which will provide current to the sensor front end. In this way the sensor front end will be heated in a pulsated manner instead of continuous heating. The next target was the introduction of pulse width modulation in the oscillator so that the oscillator should provide logic high for a small unit of time and logic low for the large unit of time in order to same maximum power. A bi-stable multi-vibrator is the circuit which has two stable states and it can remain in one state until and unless the trigger makes it go to the other stable state.

3.1.1 The feedback loop

The bi-stable function is achieved by a connection of an amplifier in the topology of positive feedback with the closed loop gain more than unity. This feedback requires the output to be fed back to the positive input in such a way that there is no phase shift between the output and the input. The basic idea of positive feedback is considered with an example

of op-amp with output going back to positive input through the voltage divider circuit as shown in Figure 3.2

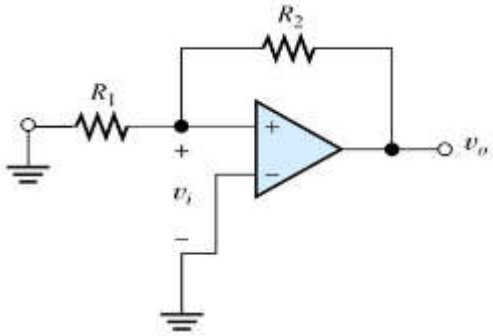

Figure 3.2 Positive feedback loop for bi-stable operation

The circuit is working without any input and there is an assumption that a small noise is there in every circuit and this noise will increase due to positive feedback to vi+. This will continue to increase until the op-amp will saturate at the positive biasing voltages. Similarly, if we start with the negative voltage, it will end in the negative biasing voltage at the end. This is also termed as Schmitt trigger in this case.

Previously both the inputs of the circuit was at ground. Now if we connect a positive source to the v_+ of the op-amp. Initially we assume that the output of the op-amp is at L_+ and hence the feedback to v_+ is βL_+. Now as the voltage at positive terminal of op-amp increases from zero volts, the output remains the same until the input voltage reaches the level of v_+. As the input voltage exceeds this voltage, the negative voltage appears between the both input terminals of the op-amp. The negative voltage will be multiplied by the open loop gain of the amplifier and the output voltage will go negative. The feedback will provide that negative voltage back to v_+ which will start incrementing the output voltage until the amplifier saturates at L-.

Further if the input voltage starts to decrease, the output will remain same until the input voltage reduces further than the voltage at v_+, which will make the difference between the inputs of op-amp as positive and make the output of the amplifier positive. The positive feedback will provide this voltage to v_+ and hence increasing the output voltage until the amplifier saturates at L_+. The phenomena is shown in Figure 3.3.

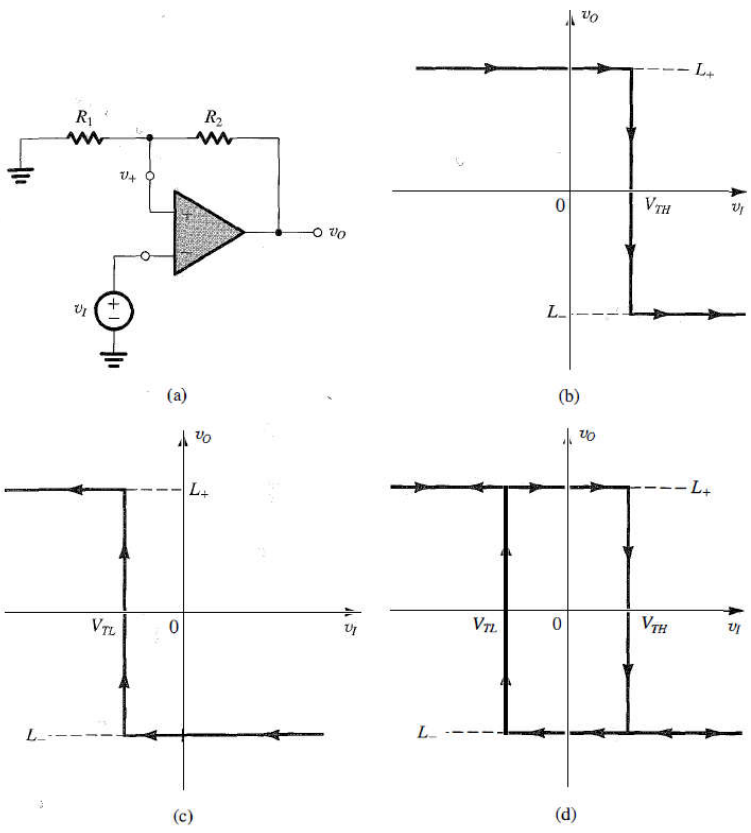

Figure 3.3 Bi-stable circuit with transfer characteristics

3.1.2 Relaxation Oscillator:

The square waveform can be produced by making the bi-stable multi-vibrator to toggle its two states in a periodic manner. The feature is produced by adding a RC circuit to a bi-stable multi-vibrator in feedback loop. This has the inverting characteristics and the output will go high and low with the charging and discharging of the capacitor. This way the

circuit has now no stable state and thus it is called astable-mutlivibrator [28]. The circuit for the astable-mutlivibrator is shown in Figure 3.4.

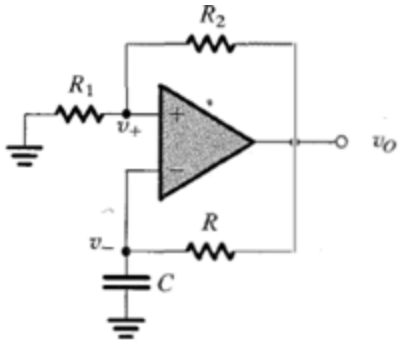

Figure 3.4 Astable Multivibrator

The operation of the circuit will be such that assume the output of the circuit is at L_+, the capacitor will start to charge to this voltage through the resistance R. This voltage will appear on v_- of the op-amp which will start to increase towards $ßL_+$ according to the time constant CR. The voltage at v_+ is already $ßL_+$ and when the capacitor voltage reaches the threshold equal to $ßL_+$, the output will switch to L_- and $ßL_-$ will appear on the v_+ terminal. The capacitor will now start discharging towards the $ßL_-$ and as soon as it reaches the lower threshold, the output toggles again and shifts to L_+. In this way, we will achieve the square output from the relaxation oscillator.

The charging time for the capacitor is given by eqaution while ⊤=CR is

$$T_1 = \mathrm{T}\ln\frac{1-ß\left(\frac{L_-}{L_+}\right)}{1-ß} \tag{3.1}$$

Similarly, the discharging time for the capacitor is given by

$$T_2 = \mathrm{T}\ln\frac{1-ß\left(\frac{L_+}{L_-}\right)}{1-ß} \tag{3.2}$$

If the charging and discharging time are equal which are obtained by $L_{+} = L_{-}$ then the time period of the square wave is given by

$$T = 2\mathrm{T}\ \ln\frac{1+ß}{1-ß} \tag{3.3}$$

3.1.3 Proposed Oscillator:

The usual oscillator of this type is based on the idea of a comparator with two bias voltages which will decide the amplitude of the output whenever the signal goes above or below these voltages. Ideal current sources supply the current to charge and discharge the capacitor. If the charging and discharging currents are equal, then the frequency of the timer will be given the formula which is not dependent upon the supply [28].

$$\frac{2I_{on}}{C_t(V_{b1}-V_{b2})} \tag{3.4}$$

These types of circuits have the problem of bias voltages and current sources, as the bias voltages should be independent of process, the fluctuations in temperature and voltage changes. The real challenge to reduce the power is to have a large time constant. This could be either achieved through the large value of capacitor and resistor, but this will not be suitable for integration. The other way is to reduce the current for charging and discharging paths in order that the capacitor would require a large time to charge and discharge which will increase the time constant. This low current can be achieved by either sub-threshold current or the leakage current. The leakage current idea explained in [29] states that it requires specific transistor to perform the leakage current. These special transistors have different gate oxide thickness and only these kinds of transistors are allowing the leakage current to flow. This solution cannot be much efficient as the leakage current is not a

constant current and with the passage of time, it may damage or degrade the performance of the device. Secondly these special transistors may not be available for all kinds of technology.

So, for the proper function of the circuit, we use normal transistor biased in sub-threshold region to minimize the current for charging and discharging paths of capacitor. The other techniques are utilized as well to minimize the current which will be discussed after the Figure showing the circuit for the proposed oscillator.

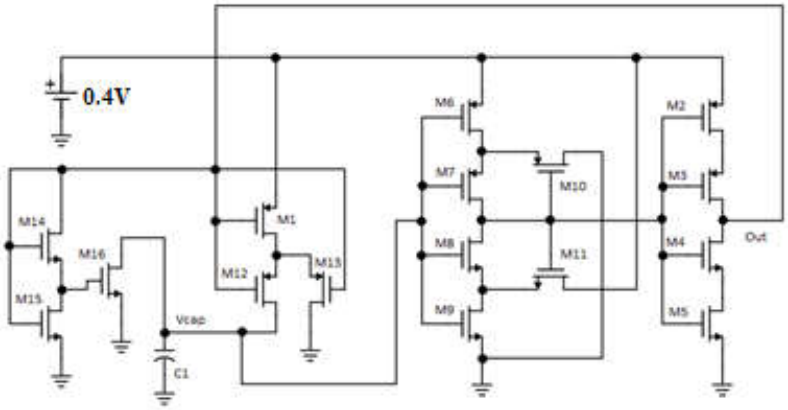

Figure 3.5 Proposed CMOS based Oscillator

The function of comparator for this purpose is performed by CMOS based Schmitt trigger instead of op-amp based Schmitt trigger to save power consumption which is the major issue of the circuit. The sections are described in detail separately along with the functions of each block.

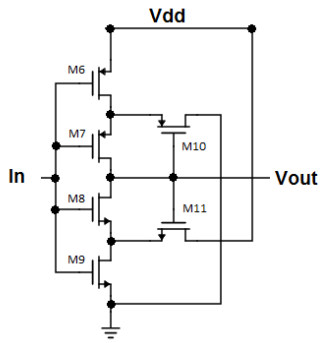

Figure 3.6 CMOS based Schmitt Trigger

The standard cascade architecture used in the CMOS Schmitt Trigger circuit design [12] is shown in the Figure 1 limits lowering of the operating voltage. The operation of the Schmitt Trigger circuit is as follows. Initially, IN = 0 V, the two-stacked p-MOSFET (M6 and M7) will be on. Hence OUT = VDD. When IN rises to VTN, M9 is on. But M8 is still off since M11 is on and source voltage of M8 is VDD. Now both M8 and M9 are on, OUT approaches to 0V rapidly and M11 becomes off. When IN approaches VDD, the two-stacked n-MOSFET (M8 and M9) will be on. Hence OUT =0. When IN falls to |VTP|, M6 is on. But M7 is still off since M10 is on and source voltage of M7 is 0 V. Thus, source voltage of M7 is rising with decreasing IN. When source voltage of M7 rises to |VTP|, M7 is on. Now both M6 and M7 are on, OUT approaches to VDD rapidly and M10 becomes off.

V_{OH} is the maximum output voltage and V_{OL} is the minimum output voltage. V_{hl} is the input voltage at which output switches from VOH to VOL. V_{lh} is the input voltage at which output switches from VOL to VOH. V_{hw} is called the hysteresis width.

$$V_{hl} = \frac{V_{DD} - RV_{TN}}{R + 1}$$

$$V_{lh} = \frac{R|V_{TP}|}{R+1}$$

$$V_{hw} = V_{hl} - V_{lh} = \frac{V_{DD} - R(V_{TN} - |V_{TP}|)}{R+1}$$

Where R is the ratio of n- and p-MOSFETs' transconductance parameters respectively.

$$R = \sqrt{\frac{K_N}{K_P}}$$

The threshold voltage can be calculated for MOSFET by the following equation.

$$V_{th} = V_{t0} + \gamma\sqrt{|-2\phi_F + V_{SB}|} - \sqrt{|2\phi_F|}$$

Where

$$\gamma = \left(\frac{t_{ox}}{\varepsilon_{ox}}\right)\sqrt{2q\varepsilon_{si}N_A}$$

V_{SB} is the source-to-body substrate bias, $2\phi_F$ is the surface potential, and V_{t0} is threshold voltage for zero substrate bias.

The CMOS based Schmitt Trigger is biased in threshold voltage. Input to the Schmitt trigger is the capacitor voltage which is either charging or discharging shape. The Schmitt trigger is based on inverter circuit and when charging input is there the output is logic zero and when discharging output is there the output is logic one.

The next stage for the Schmitt trigger is the inverter to maintain the positive feedback in order maintain the oscillations. The output of the inverter is fed back to the transistors as switches which will allow v_{dd} and gnd to connect to the capacitor and the charging and

discharging. The charging of the capacitor is carried out through PMOS which will be on when it gets the output low from the feedback circuit. When the PMOS turn on in sub threshold region, in order to get the long off time for the output, the charging current is further divided into two unequal paths by two parallel PMOS transistors M12 and M13 which will pass the smaller ration of current to charge the capacitor through M12. This will increase the off time up to 40 seconds with the capacitor value of 100pF. Similarly, the discharging path is turned on by NMOS and size of NMOS is kept bigger than PMOS in order to have smaller time for discharge so that the output will be on for a smaller time according to the requirement. M14 and M15 serves as voltage divider to provide the required voltage to M16 to provide the suitable discharging time of capacitor. To alter the time size of M14 and M15 is changed until the required results are obtained.

The charging and discharging time of the oscillator can be changed by varying the size of charging and discharging path switching transistors. The maximum half period we are getting with 100pF capacitor is around 44 seconds. For the applications which require more time period, a capacitor can be added in parallel with 100pF capacitor which would increase the time period of the oscillator.

In sub threshold operation, the current through MOSFET is the exponential function of Vgs and Vds and is given by

$$I_{D-subthreshold} = I_o e^{\frac{V_{GS}-V_{TH}}{n\emptyset_t}} \left(1 - e^{\frac{-V_{DS}}{n\emptyset_t}}\right)$$

$$I_o = \mu_o C_{ox} \frac{W}{L} (n-1)\emptyset_t^2$$

$$\phi_t = \frac{KT}{q} \approx 26mV$$

If $$V_{ds} > 3\phi_t \approx 78mV,\ \left(1 - e^{\frac{-V_{DS}}{\phi t}}\right) \approx 1.$$

The charging current through M1 is calculated first. As V_{ds} is greater than 78mV so the effect of V_{ds} will be eliminated in the calculation of current and will only depend upon the V_{gs} of M1. This will be the total current through M1 which is split in two branches with PMOS with unequal sizes to divide the current in such a way that less current goes towards the charging of capacitor. $(W/L)_{M13} > (W/L)_{M12}$

$$I_{M1} = I_{M12} + I_{M13}$$

The charging current can be found directly by taking the ratio of sizes of transistors or by substituting the values in above equations to find the both currents separately. The Charging current will be taken as average because it is maximum when the capacitor is uncharged and it goes less when the capacitor is charged to the maximum value.

Similarly, for discharging of capacitor, NMOS block consisting of M14, M15 and M16. The gate voltage of discharging transistor M16 is divided by two transistors M14 and M15 in order to reduce the discharging current and increase the discharging time for the capacitor. V_{gs} can be calculated by taking the ratios of sizes of M14 and M15. The current can be found through the current equation in subthreshold. Here again the V_{ds} is larger so effect of V_{ds} will be neglected.

The charging and discharging times can be calculated by the following equations. During the charging time the output is low while during discharging period the output is high.

$$T_{Charging} = \frac{C_l V_{hl}}{I_{Charging}}$$

$$T_{Discharging} = \frac{C_l V_{lh}}{I_{Discharging}}$$

Total time for one period will be

$$T_{tot} = T_{Charging} + T_{Discharging}$$

Frequency of the timer can be determined from the time for one period of oscillation.The sizes for all the transistors in the circuit is given in the following table.

Table 3.1 Sizes of the transistors in Oscillator

Transistors	W/L
M_1, M_2, M_3, M_4, M_5, M_{10}, M_{11}, M_{12}, M_{14}, M_{16}	320n/150n
M_6, M_7, M_8, M_9,	1u/1u
M_{13}	5.63u/150n
M_{15}	3.5u/1.5u

The output waveform of the oscillator is shown in next chapter of results and discussions.

3.2 Voltage Dividers

The sensor is using different circuit blocks which requires different supply voltage. To use the same supply for the whole circuit, a 1V supply with two voltage dividers based on NMOS are utilized. The first one gives the output of 0.6V by adjusting the sizing of these

transistors. The second voltage divider takes the 0.6V and provides 0.4V by sizing the transistors properly. The 0.4V is utilized by sub-hertz oscillator and 0.6V is utilized by the buffer. Rest of the circuit works with 1V supply.

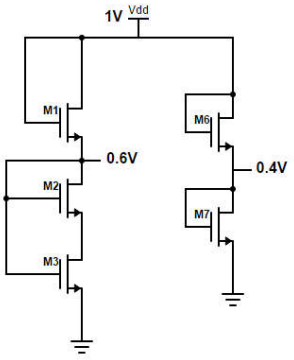

Figure 3.7 Voltage dividers for the circuit

3.3 Buffer

In order to drive all the circuits with this timing oscillator, the digital buffer is required. This buffer performs two functions, one is to provide the function of buffer and second is the voltage level shifting from 0.2V to 0.6V for the proper operation of transistor switch in strong inversion. The inverter used in the oscillator is cascaded with another one in order to give the output as buffer. The difference between the normal inverter based buffer and this one is that it is changing the input signal of 0.4V amplitude to 0.6V output. The first inverter is having the supply voltage of 0.4V while the 2^{nd} stage is having the supply voltage of 0.6V. These voltages are generated from the main supply of 1V. All the transistors from M17 to M24 are in sub-threshold region with minimum W/L of 320n/150n. The buffer is shown in Figure 3.8

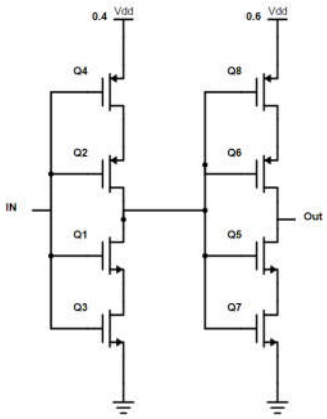

Figure 3.8 Inverter based buffer

3.4 Wheatstone bridge

The sensor front end is connected in the topology of Wheatstone bridge in order to get maximum sensitivity although by differential mode, 2 resistors are less and they will save the power but it has degraded sensitivity as compared to wheatstone bridge. With better sensitivity, we can detect the presence of gas earlier than the differential circuit and this will save the power by not heating the sensor to full 400°C. As the major cause of power consumption is the micro-heater heating the sensor.

The R_2 is the gas sensitive resistor which has catalyst applied over the surface and R_3 is the resistor with no catalyst. Different values of resistances are used in literature for the sensor front end. This mainly depends upon the material used to fabricate the micro-heater and that will have its specific resistance. So, in literature the values of Ω, KΩ and MΩ are used [8], [21], [27] and we have tested the bridge for all these ranges of resistances. In the presence of gas, the gas sensitive resistor can change the resistance up to twice depending upon the material being used to create these resistances. Even in low resistance case it might increase more than twice [8], so we have analyzed the change of resistance right

from the start of 1% to 100% and even more in case of low resistances. The results are discussed in next chapter of results and discussion. The Wheatstone bridge configuration is shown in Figure 3.9.

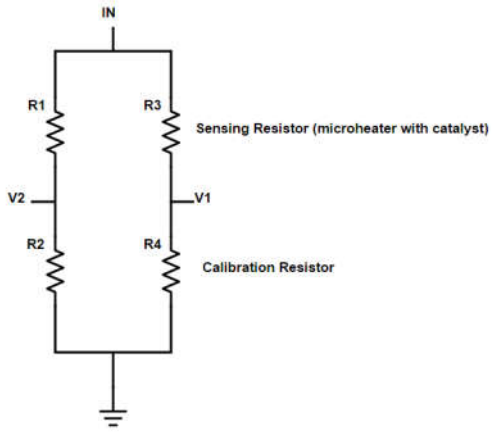

Figure 3.9 Wheatstone bridge configuration of sensor front-end

3.4.1 Micro-heater for gas sensor

Micro-heater is an essential part of gas sensor as it must heat the resistor to the required temperature to sense the presence of gas in the surrounding atmosphere. These micro-heaters are fabricated with different materials and different designs to get maximum efficiency of heating with minimum power consumption. The basic configuration of a typical micro-heater is shown in the Figure 3.10.

The main block consists of two resistors baked inside a single housing. One of them is the heater resistor R_h which heat up to the required temperature when the current pass through it and the heat of this resistor is passed to the resistor which is connected for the measurement in the circuit. Catalyst is applied over the surface which burns in the presence of gas which changes the resistance of the gas sensing resistor R_s [30], [37-38]

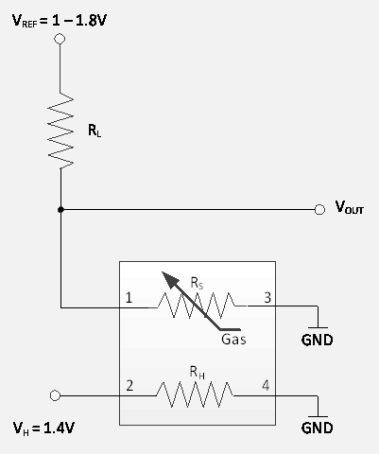

Figure 3.10 Typical micro-heater

The design of micro heater is vastly present in the literature which have a huge diversity in shape, size, patterns and materials in order to have maximum resultant heating with minimum power consumption. Still today the power consumption of these micro-heaters is in mW [31-33]

3.4.1.1 Geometries of micro-heater:

The micro-heaters are fabricated in different patterns to get the desired performances as there are different kinds of heat loss through conduction, convection and radiation phenomena. Some of the shapes are described briefly here as

- **Plane plate structure with hole in center:** By this design, the process of natural convection takes place. Due to the hole in the center of the structure, the problem of uneven and random appearance of hot spots near the center and the power consumption of these structure is high. The structure is shown in Figure 3.11.

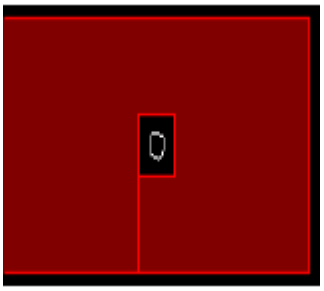

Figure 3.11 Plate structure of micro-heater with hole in center

- **Meander line structure:** These structures have 90° turns for the meandering structure which takes a small area instead of a straight-line structure. The problem with this structure is the creation of hot spots with high temperatures around the bends which will cause uneven heating. The structure is shown in Figure 3.12.

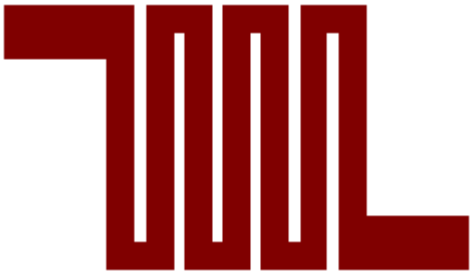

Figure 3.12 Meander line structure

- **Double spiral shaped:** Due to the problems of meander design of micro-heater, a double spiral shaped micro-heater were created with variable gap between the lines and variable widths of the line inside the pattern. The shape is shown in the Figure 3.13.

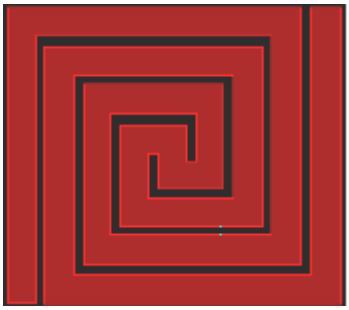

Figure 3.13 Double Spiral Shaped

- **Fan shaped Micro-heater:** The modification of double spiral shaped micro-heater creates the fan shaped micro-heater. This design is one of the best design to achieve uniform heating along with the very low power consumption. The structure is given in Figure 3.14.

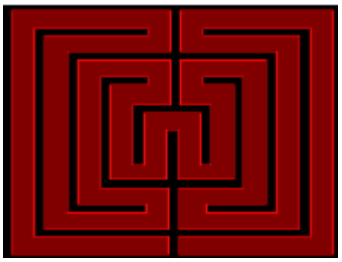

Figure 3.14 Fan shaped Micro-heater

- **Honey-comb Shaped Micro-heater:** This design of micro-heater allows the redistribution of thermal energy and provides the uniform heating profile. The structure is given in Figure 3.15.

Figure 3.15 Honey-comb Shaped Micro-heater

- **S-Shaped Micro-Heater:** This design is also very suitable for the low power consumption and uniform heating but is only used for small sized sensing structures. The structure is given in Figure 3.16.

Figure 3.16 S-Shaped Micro-Heater

3.4.2 Noise analysis of Wheatstone bridge:

In several applications, Wheatstone bridge with resistive bridge elements constitute the front end and are excited using the DC supply and the reading is taken at very low frequency. Although all resistive elements exhibit small amount of Nyquist noise but in this particular case, 1/f noise will dominate and will be the biggest source of noise as you will go low in frequency.

The solution of this problem to avoid 1/f noise is to excite the bridge using AC. The frequency of AC should not be very high and it will be cleared in next section that what minimum frequency of AC will solve the problem of 1/f noise. Following are the types of noise that effects the resistive Wheatstone bridge.

3.4.2.1 Nyquist Noise:

Nyquist noise also known as thermal noise exists in both AC and DC excitation for resistive bridge measurement circuit. This is due to the motion of particles (electrons) inside the resistance which does not depends upon any supply voltage. The response of

such noise has white spectrum and it exists in all the frequency bands. The effect of this noise cannot be removed completely but it can be reduced by decreasing the bandwidth.

3.4.2.2 Shot Noise:

Whenever the current flows through the resistor, the noise may appear in the form of an opposing voltage which is termed as shot noise. It occurs due to random fluctuations in the flow of current. In order to avoid this noise, we must avoid the large amount of current through the resistors which will result in the presence of shot noise.

3.4.2.3 Flicker Noise:

The flicker noise of 1/f noise typically exists in the electronic systems at low frequencies, normally when we go below 100 Hz. As there is inverse relation between the noise and frequency so it rises with the decrease of frequency towards DC. The sources of this noise are random fluctuations in any parameter of the circuit.

So, combining all the facts the noise spectrum for the resistive network is shown by the Figure 3.17 [34]

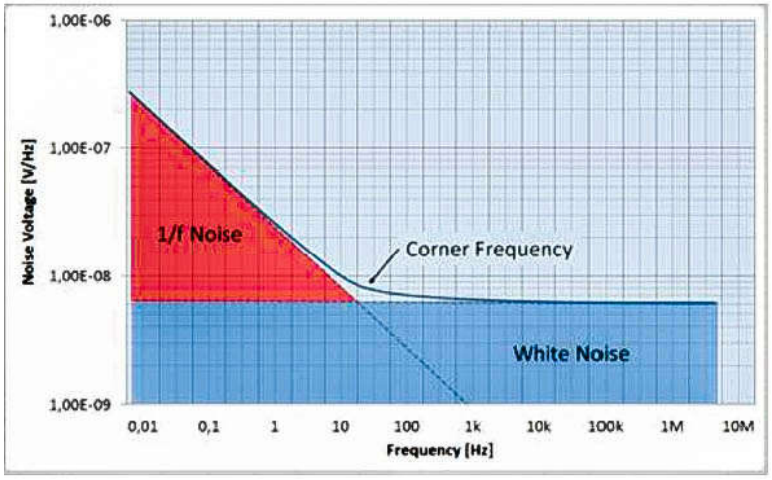

Figure 3.17 Noise spectrum for resistive circuit

3.5 Oscillator for excitation of Wheatstone bridge

After the noise analysis of Wheatstone bridge, we should excite the bridge using AC instead of DC to save from 1/f noise. The sinusoidal waveform generators are the most suitable waveforms for this purpose as it has a single frequency and has no offset [35]. But the sine wave generators require a start-up circuit for the implementation and that requires the complex circuitry for this task. So, in order to simplify this block, we use the same oscillator which we have used previously with a little modification.

The circuit for this block will run from 1V supply instead of 0.4V to get the maximum output swing in order to supply it to the bridge circuit. The output of the oscillator is a square waveform which has many frequency components in it and may cause some problems while we supply that to the Wheatstone bridge. To solve this issue, we supply the capacitor voltage to the bridge circuit in order to take the measurement. The charging discharging waveform is AC and the frequency of oscillation is around 1 KHz to save from the 1/f noise.

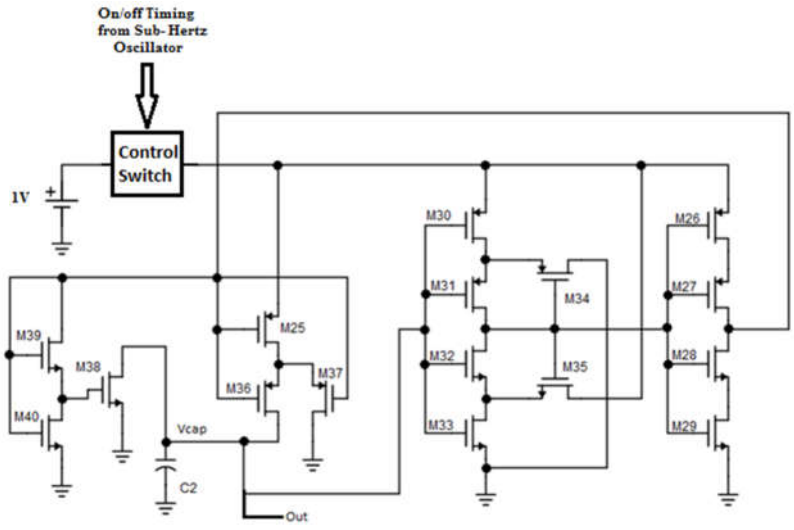

Figure 3.18 1 KHz oscillator for Bridge excitation

The capacitor for this oscillator is 5pF and the output is taken from the capacitor node which will supplied to the next stage. The W/L ratio of these transistors are given in the table 3.2

Table 3.2 Sizes of 1 KHz oscillator circuit

Transistors	W/L
M_{25}, M_{26}, M_{27}, M_{28}, M_{29}, M_{34}, M_{35}, M_{36}, M_{38}, M_{39}	320n/150n
M_{30}, M_{31}, M_{32}, M_{33}	1u/1u
M_{37}	10u/1u
M_{40}	320n/200n

The output waveform is show in next chapter with title of results and discussions. The same phenomena of PWM is used to control the charging and discharging time for the capacitor but here the charging and discharging time are almost equal.

3.6 Analog Buffer

In order to supply the AC waveform, form the oscillator to bridge circuit, analog buffer is required in order to avoid the oscillator from loading effect. The analog buffer is based on simple two stage op-amp, with PMOS as differential input stage. This stage gives the open loop gain of 40dB with power consumption in nW. When connected in closed loop for buffer, it gives the loose and not performing as a proper buffer. So, in order to enhance the gain and better performance, a CS stage is added and the buffer configuration is achieved.

Input waveform from the oscillator stage is buffered and applied to the wheatstone bridge for the measurement. The op-amp buffer is shown in Figure 3.19.

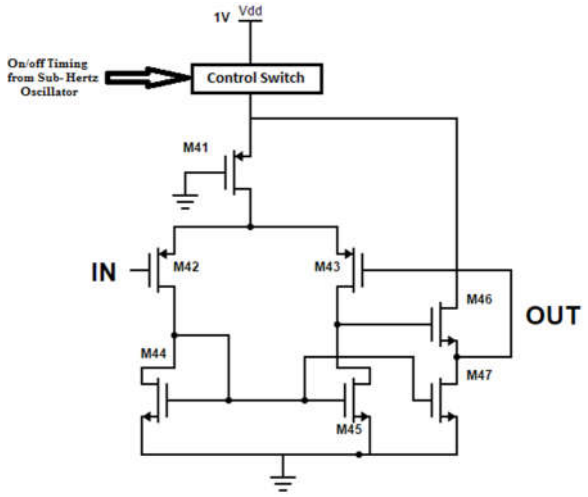

Figure 3.19 Analog buffer based on two stage op-amp

As the input signal has a DC offset due to the type of input signal which is the charging and discharging waveform between the upper and lower thresholds. The offset in the input is always multiplied by the gain and that offset appears in the output. As the op-amp is used as a buffer so its closed loop gain is around one and the DC offset almost remains the same after passing through the buffer stage. The W/L for the buffer circuit are given in the table 3.3.

Table 3.3 Sizes for the Analog Buffer

Transistors	W/L
M_{41}, M_{47}, M_{44}, M_{45}	1u/1u
M_{42}, M_{43}	1u/700n
M_{46}	50u/1u

3.7 Difference Amplifier:

When the Wheatstone bridge is excited with the AC signal from the oscillator through buffer, it enters both the branches of Wheatstone bridge with equal impedance and the differential output of the bridge will be zero in this case. When the gas is present, the resistance of the gas sensing resistor will change which will cause the output of that branch of Wheatstone bridge to change and the differential output of the Wheatstone bridge will not be zero. This would be a very small value and will be difficult to monitor for every small change like 1% in the resistance. In order to get the difference from the outputs of Wheatstone bridge amplified, the difference amplifier is used based upon op-amp.

The main idea is to have much more gap between every 1% change of resistance that it can be easily monitored. For that purpose, we require a high closed gain from the amplifier. This may cause a power consumption but still we will be able to detect the gas at very early stage as compared to the detection after a specific amount of time. The power consumption of such circuits is usually in hundreds of microwatts which will be still better than using the micro-controller with mW of power consumption.

The difference amplifier is used to take the difference between the input signals and rejects any common signal to both of them. An ideal difference amplifier should have the zero-common mode output and a fixed gain output in differential mode [28]. The output of the difference amplifier is given as

$$v_o = A_d v_{id} + A_{cm} v_{icm} \tag{3.5}$$

Where A_d is the differential gain, v_{id} is the differential input, A_{cm} is common mode gain and v_{icm} is common mode input for the amplifier. The amplifier we are using is the two

stage op-amp with input differential stage implemented with PMOS transistors and the second stage with a common source amplifier. The ratio of resistors for the feedback path to input path is 70:1 such that we are getting the gain of 63.5 for the output signal. The input signal is has the full scale change from 0.0798mV to 7.412mV when the resistance change is from 1% to 100% for which the output will have the range from 5.067mV to 471.36mV for the same amount of change. The circuit for the difference amplifier is shown in Figure below. The input is having the offset of around 30mV which is reduced by negative feedback but the remaining one is multiplied by the gain and appears in the output. When the difference of resistance occur, it also changes the amplitude as well as the offset in the particular branch of Wheatstone bridge. So the inputs going to difference amplifier have different amplitudes as well as different offset. The supply voltages are 1V and -1V.

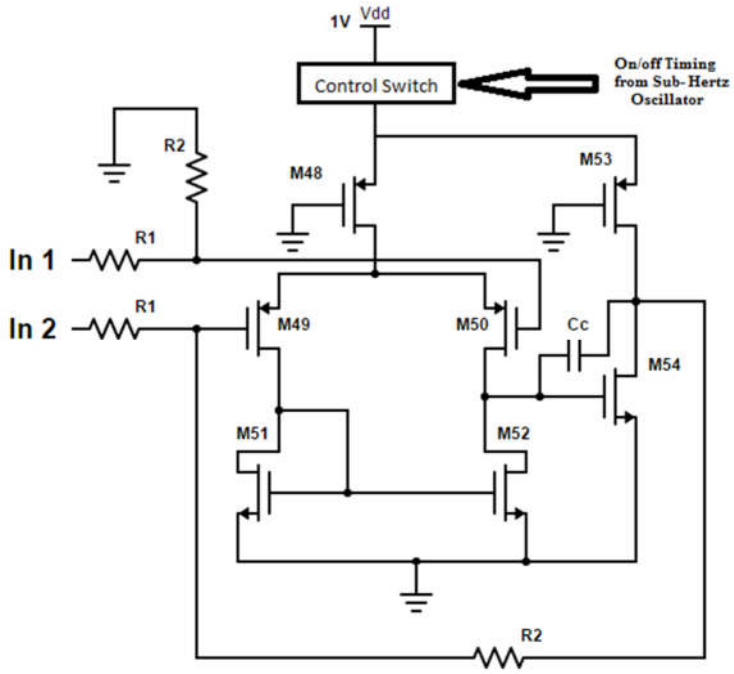

Figure 3.20 Difference Amplifier

The sizes for these transistors are shown in table below. These values are selected in order to make all the transistors in pinch-off mode in order to get maximum gain out of the amplifier so that the output may have a large variation with the change in input.

Table 3.4 Sizes for the difference amplifier

Transistors	W/L
M_{48}, M_{53}, M_{54}	10u/700n
M_{49}, M_{50}	10u/1u
M_{51} , M_{52}	12u/1u

The output waveforms will be discussed in detail in the next chapter of results and discussions as well as the comparison tables and graphs will be displayed.

3.8 Switching Transistors

In order to make all the circuit working only in the time when the sub-hertz oscillator have logic level high, the switches based on transistors are used. Although a single transistor can be used as a switch like NMOS where the drain is connected to supply and gate to the control signal and source to the circuit where the supply has to be delivered. But taking the output from source will not give the efficient results. So in order to maintain the efficiency a combination of NMOS and PMOS are used where NMOS is used as common source and PMOS as common drain. This combination allows the perfect switch and maximum power transfer. The switch is shown in Figure below

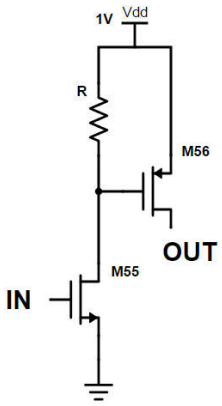

Figure 3.21 Transistor Switch

3.9 Operation during the presence of gas

During the normal operation of gas sensor with no gas, the output of the difference amplifier will be almost zero. The nominal heating time for the microheater varies between 0.4sec – 2.5sec [8], [36]. The nominal time it takes to cool down back to the IC temperature takes 0.2 sec to 2sec depending on the construction of microheaters [36-37]. Normally these gas sensors are operated once between 20sec- 60sec depending upon the location and type of gas being monitored. The readings are taken keeping the above timings in considerations so for experiment, the on time for sensor for heating is chosen close to maximum time that is 2sec and 44sec for sleep time provided by sub-hertz timer. During this time, not only microheater, but the whole circuit is turned off as the supply to all the circuit goes through the switch operated by the same sub-hertz timer. The power consumption will only for the time of operation of the circuit and average power consumption is calculated for the whole period.

The output of difference amplifier with the amplitude and offset will depict the presence of gas and the reading will be sent to receiver end where the reading would be analyzed

and return the status to continue the operation if the gas is not present. Later, when the gas will be present, the output will be shown so in order for the safety of the location, the sensor will not take the reading after 40 seconds but instead it will continue to take the reading until and unless the presence of gas is eliminated [40]. In order to propose this feature for future, a comparator with output connected to switches consisting of NMOS and PMOS with gates connected together for input will be added. The drain of NMOS is connected to the main supply while the PMOS is connected to the output from sub hertz oscillator. When the gas will not be present output will be zero and PMOS will be on to supply the normal sub hertz on time for the sensor but when the gas will be present the output will turn on NMOS and turn off PMOS and sensor will be connected directly to the supply for continuous mode of operation until the sensor is reset or if the gas eliminates from the premises.

CHAPTER 4

RESULTS AND DISCUSSIONS

This chapter will discuss the results and discussions for the blocks described in previous chapter. The output waveform of each block will be separately and also the required conditions will be discussed. The comparison tables along with the different graphs will also be displayed.

4.1 Output of Sub Hertz Oscillator

The sub hertz oscillator is working with the voltage of 0.4V and all the transistor are in sub-threshold region. The capacitor used is of 100pF in order to get the frequency of 0.0217 Hz. In order to get more low frequency, the capacitor in parallel have to be added. The charging time for the capacitor is 44 seconds which will keep the output low for this time and discharging time for the capacitor is 2 seconds for which the output will be high.

The Schmitt trigger sets the upper threshold voltage at 68.9 mv while the lower threshold is kept at 20.32 mv keeping the capacitor voltage to swing between these thresholds and maintaining the output amplitude of 48.58mV for the capacitor voltage. The output of the oscillator switches between 0V and 216.5 mV. The output waveform of oscillator and the capacitor voltage is shown below

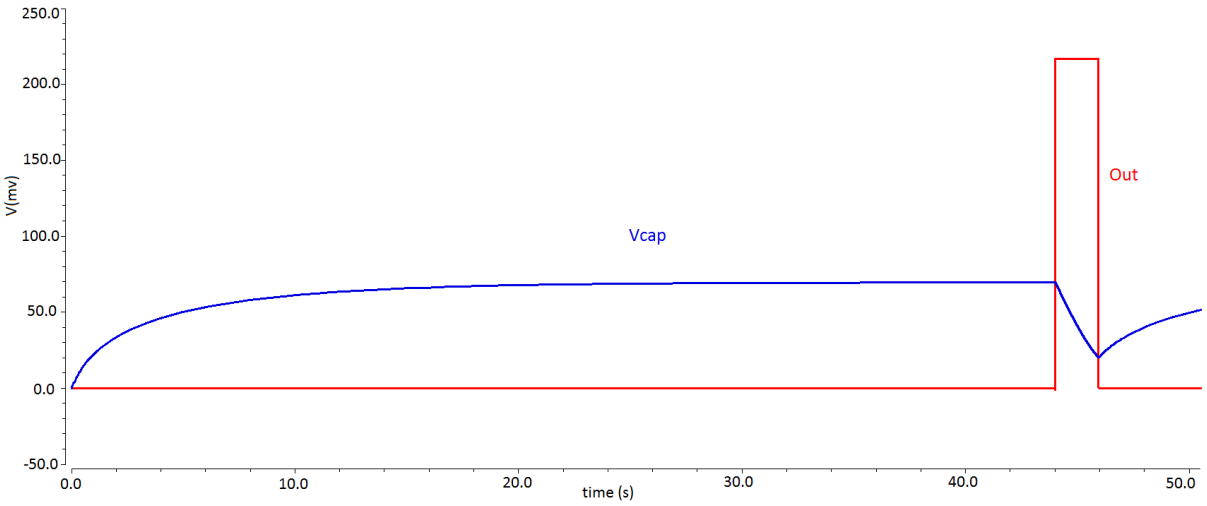

Figure 4.1 Output Characteristics of Sub-Hertz Oscillator with C=100p

By changing the value of capacitor to lower value, we can get a fast response for the oscillator and by changing W/L of charging and discharging paths we can adjust the PWM as well. Now making the value of capacitor as 50pF and frequency of oscillation changes to 0.05Hz. This phenomenon can be adapted for the sensors which are located in the sensitive areas and they require getting the reading faster as compared to the other places. The output characteristics with half the value of capacitor is shown below.

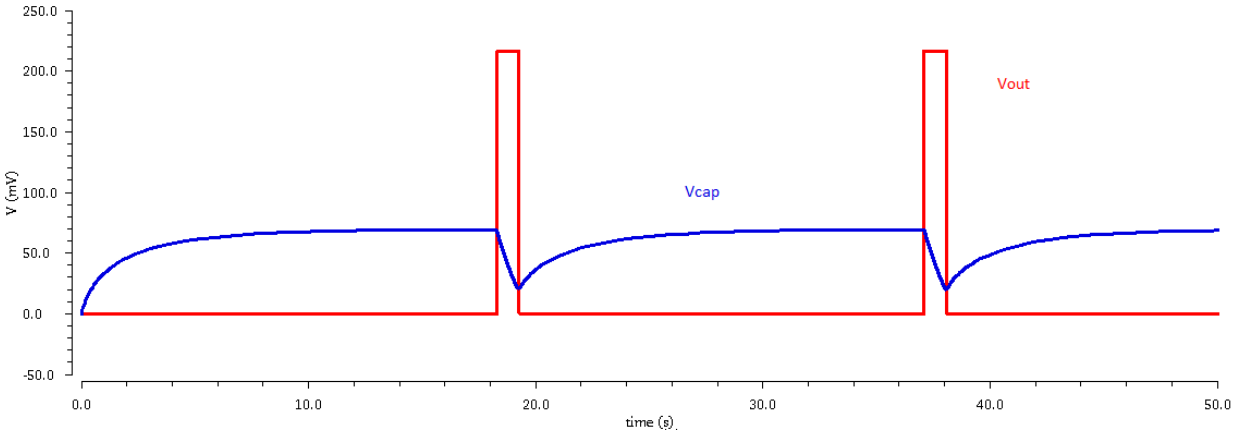

Figure 4.2 Output Characteristics of Sub-Hertz Oscillator with C=50p

4.2 Output at Buffer Stage

The next stage of oscillator was the digital buffer in order to provide the output of the oscillator to later circuit with the amount of voltage which can be served to turn on and off the transistor in linear or pinch-off region. The inverter based buffer uses the 0.4V for the first inverter and 0.6V by the second buffer. The input to the buffer is the square waveform with values of 0V and 216.5mV while the output from the buffer is between 0V and 600mV. The output at the buffer stage is shown in Figure 4.3.

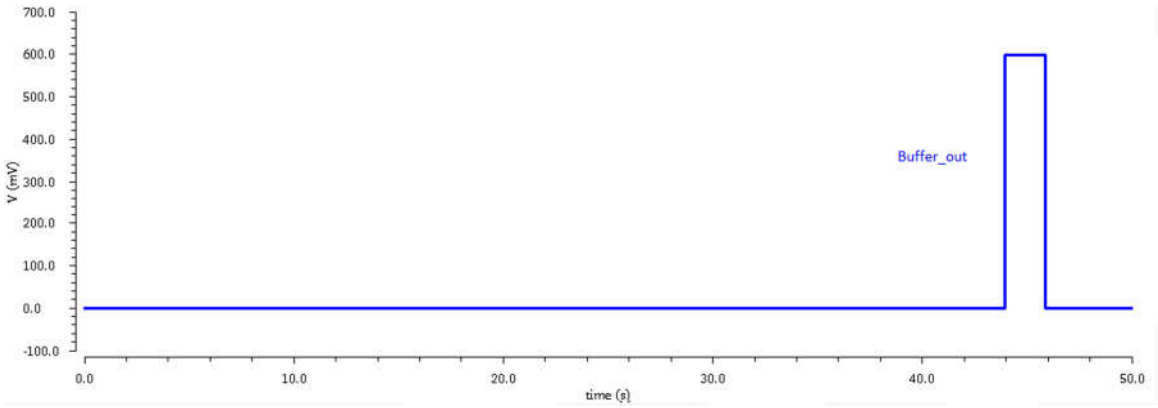

Figure 4.3 Output characteristics at buffer stage

This output is supplied to the switches to turn on the other parts of circuit during this time and for the other time, all the other circuits should be off in order to save the power.

4.3 Characteristics of 1 KHz oscillator:

The output of buffer is applied to switch which connects the 1 KHz oscillator with 1V supply voltage and it starts giving the output. The value of capacitor is 5pF for this oscillator. We make the charging and discharging paths equal in order to get a proper output waveform.

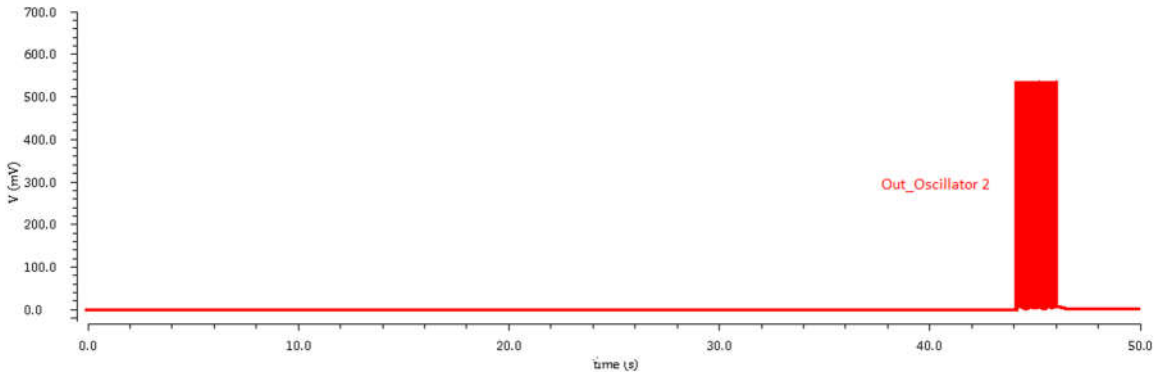

Figure 4.4 Output of 1 KHz Oscillator

Zooming that waveform, we get the output of the oscillator as follows

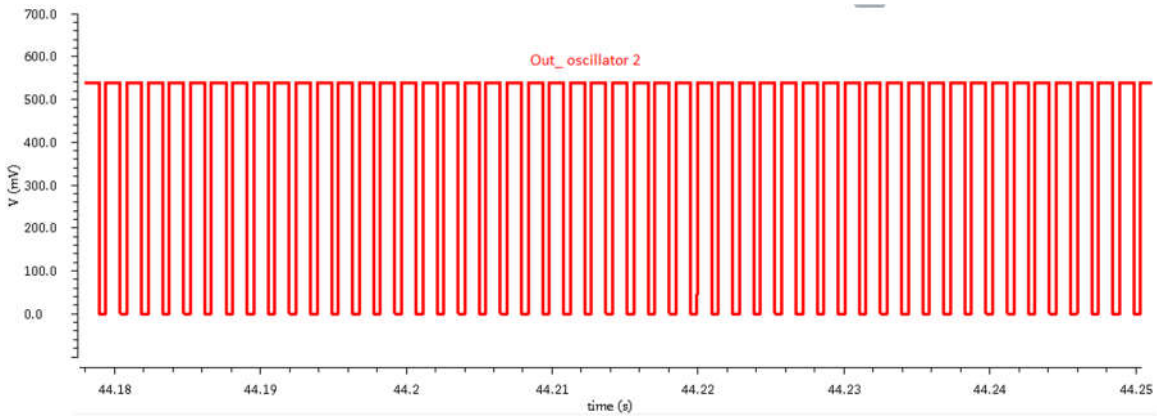

Figure 4.5 Zooming in the waveform of 1 KHz oscillator

The frequency comes out to be around 1 KHz for the oscillator but we have to use the capacitor voltage of this oscillator to be used as output for the next stage to excite the Wheatstone bridge. So, the capacitor voltage waveform with same frequency is given by the following Figure 4.6. The waveform has the offset of about 100mV while the swing is between 130mV to 68mV making the amplitude of the capacitor voltage to be around 62mV.

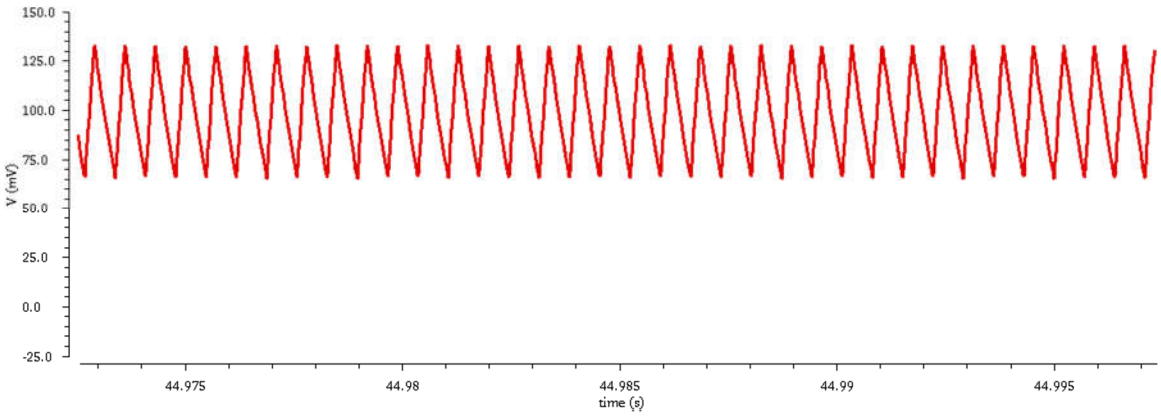

Figure 4.6 Capacitor voltage for the 1 KHz oscillator

4.4 Characteristics of Analog Buffer Stage

The next stage after the 1 KHz oscillator will be the analog buffer in order to provide the capacitor voltage to the load of Wheatstone bridge and avoiding any loading effect on the oscillator. The op-amp based oscillator was designed in order to get the required buffer output. The buffer is working from the supply voltage of 1V. The supply is reaching it through the switch which is controlled by the sub hertz oscillator which will only allow this buffer to work during the required time and for other time it is off. The waveform of previous stage from capacitor and the waveform of analog buffer are shown in the Figure 4.7.

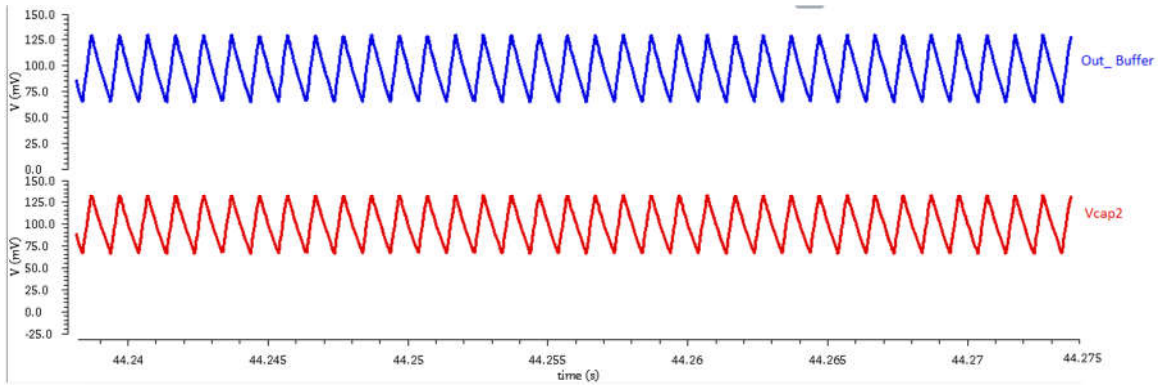

Figure 4.7 Output waveform of Analog buffer compared with capacitor voltage

4.5 Characteristics at Wheatstone bridge:

The output of the buffer stage is then supplied to the Wheatstone bridge with two normal resistors and two micro-heater based resistors among them one is gas sensitive due to the catalyst present on the surface of that resistor. When no gas is present, all the resistors have same values so the overall differential voltage from the bridge will be zero and both voltages will be same in magnitude.

When the gas is present, the resistance of gas sensing resistor will change and the differential output from the Wheatstone bridge will not be zero. Both voltages will have different amplitude as well as different offset voltage. In the literature, different values of resistances are used for Wheatstone bridge depending upon the resistance of micro-heater based resistor which is constructed from different materials have resistance in different ranges. The other resistors are selected according to the resistance of micro-heater based resistor.

The outputs from both branches of wheatstone bridge is given in the Figure 4.8 when no gas is present and all the resistors have the same value of 1KΩ.

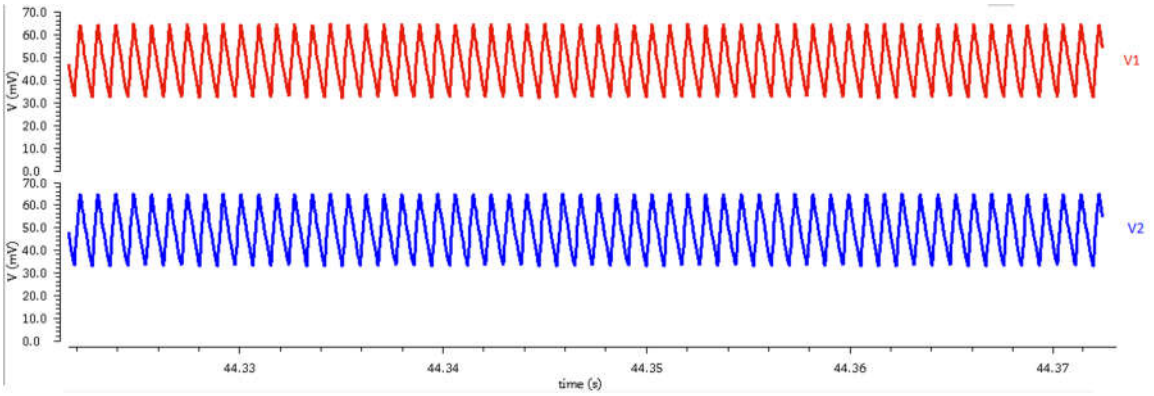

Figure 4.8 Outputs of Wheatstone Bridge at equal transistors of 1KΩ

When the gas is present and resistance of gas sensitive resistor changes. The full-scale variation is given when the resistance becomes twice of the initial value for the gas sensitive resistor. In that case, the gas sensitive resistor has resistance of 2KΩ and other three resistances are of 1KΩ. There will be change in the amplitude for both the branches of Wheatstone bridge as well as the offset voltage will be different. The output waveform for the configuration is given in the Figure 4.9

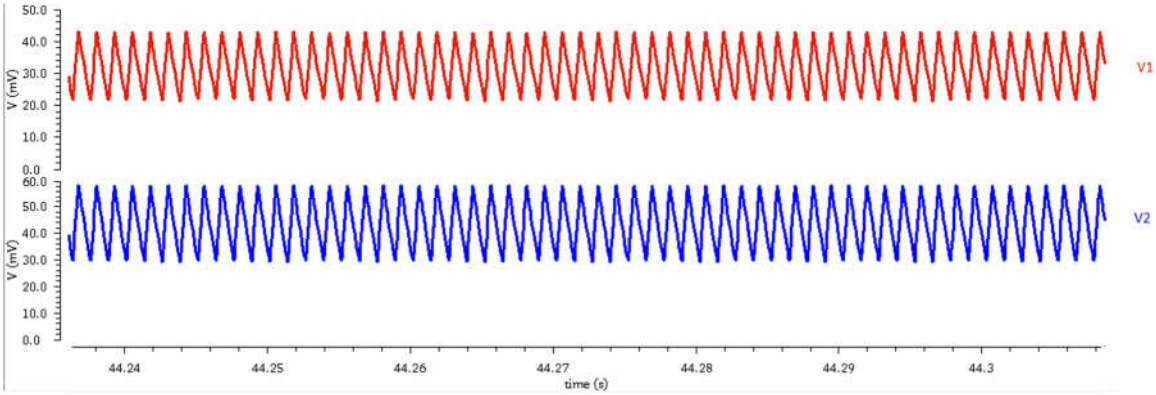

Figure 4.9 Outputs of Wheatstone Bridge at 1KΩ and 2KΩ resistors in one branch

The values of these voltages and the output obtained is discussed in next section with complete table and waveforms.

4.6 Output Characteristics of Gas Sensor:

The output of the gas sensor is evaluated at the output of the difference amplifier. For the catalytic sensors, during the presence of gas, the resistance of the microheater based resistor increases while for the semiconductor based microheater, the resistance decreases with the presence of gas. The output with each case is evaluated and in the end the comparison table will be shown. First the outputs for the KΩ range will be discussed and the waveforms will be shown.

- **Case 1:** When the bridge is constructed with KΩ resistors, we choose 1KΩ for both resistance for the normal resistors and 1KΩ for the micro-heater based resistors. When no gas is present, no change for the gas sensitive resistor takes place and both the outputs of Wheatstone bridge will have a little difference of offset as they are directly connected to difference amplifier but the amplitude will be same. The output for the difference amplifier will be a very small voltage due to common mode gain which is ideally zero but practically not. The output is around 2mV for the inputs of 26.182mV.

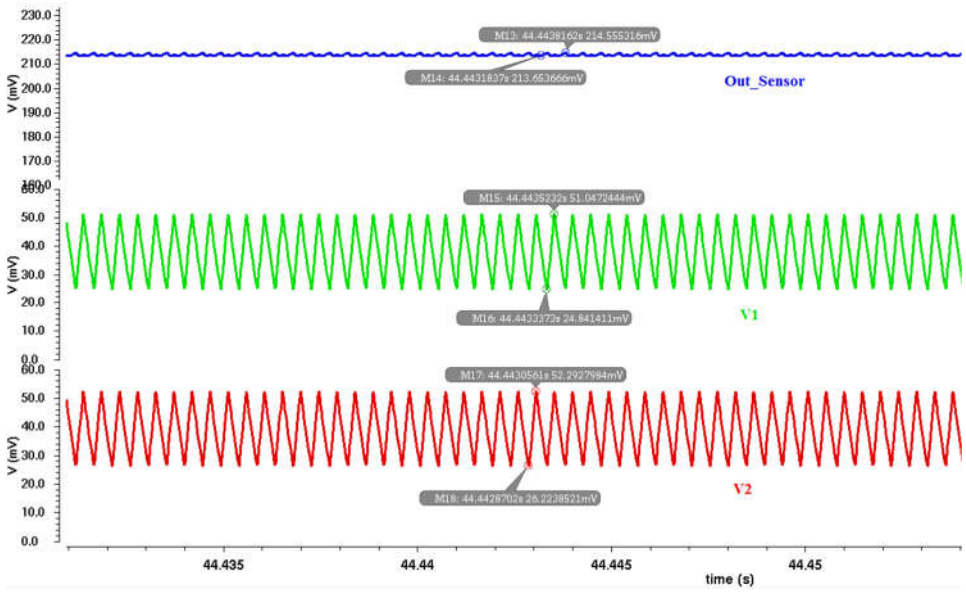

Figure 4.10 Output for the case of both 1 KΩ Resistors

- **Case 2:** When the gas is present and the resistance of the gas sensitive resistor starts to change. For increase of 1% of resistance, the change at the output of wheatstone bridge is 0.125mV and the output will be 5.439mV having 43.5 gain from the difference amplifier. The offset for the output waveform is 207.3mV. The output waveform is given in Figure 4.11.

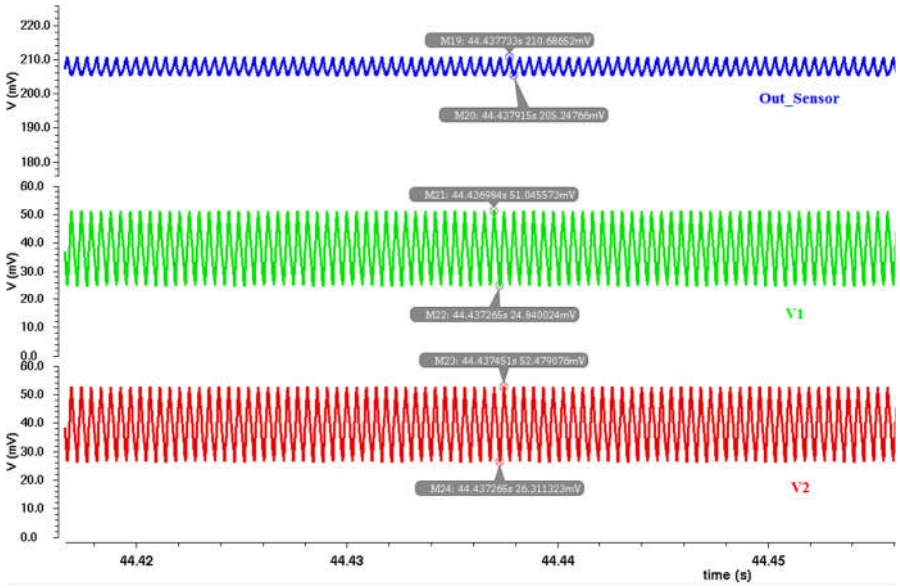

Figure 4.11 Output for the case of increase of 1% resistance

- **Case 3:** For increase of 5% of resistance, the change at the output of wheatstone bridge is 0.433mV and the output will be 18.854mV having 43.5 gain from the difference amplifier. The offset for the output waveform is 240.2mV. The output waveform is given in Figure 4.12.

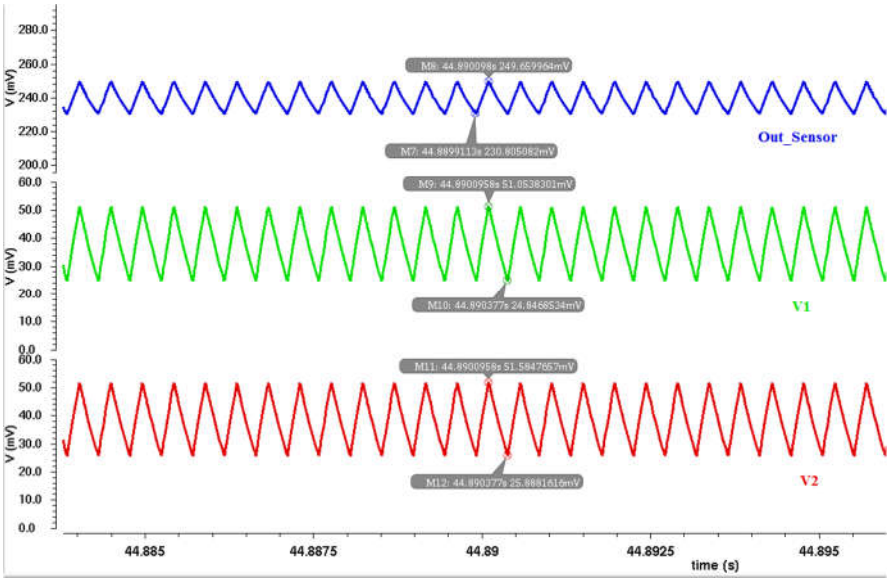

Figure 4.12 Output for the case of increase of 5% resistance

- **Case 4:** For increase of 10% of resistance, the change at the output of wheatstone bridge is 1.008mV and the output will be 43.535mV having 43.5 gain from the difference amplifier. The offset for the output waveform is 272.3mV. The output waveform is given in Figure 4.13.

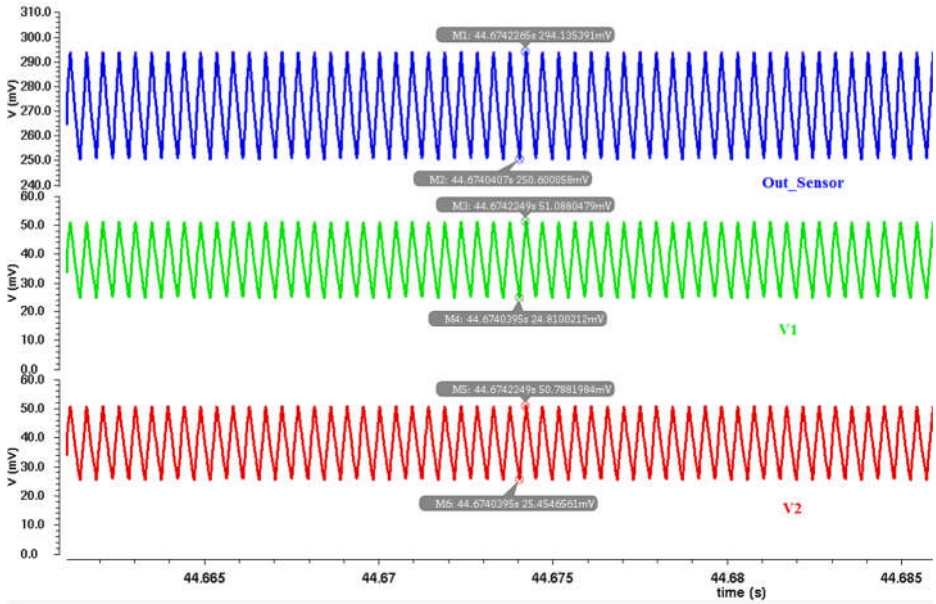

Figure 4.13 Output for the case of increase of 10% resistance

- **Case 5:** For increase of 20% of resistance, the change at the output of wheatstone bridge is 2.068mV and the output will be 90.001mV having 43.5 gain from the difference amplifier. The offset for the output waveform is 332.7mV. The output waveform is given in Figure 4.14.

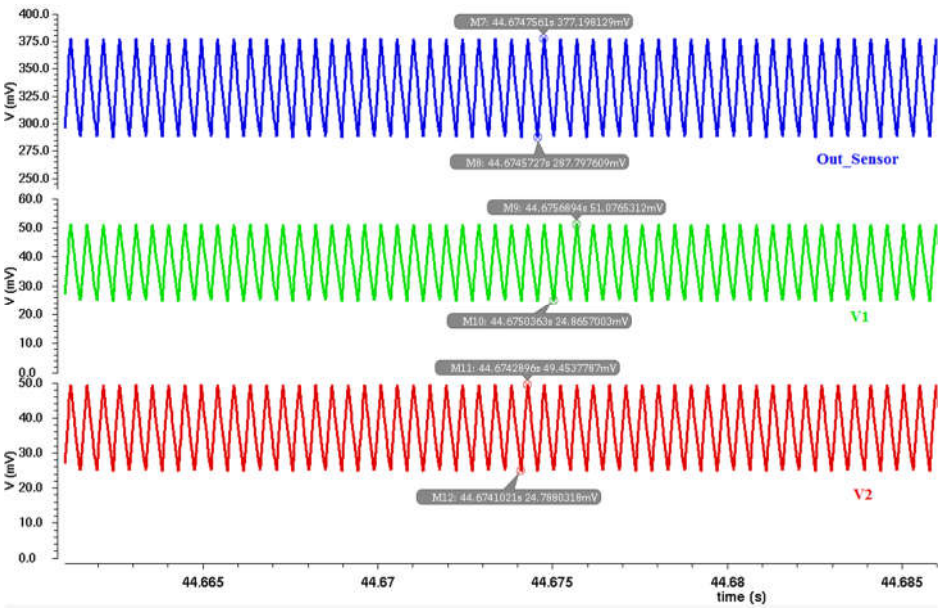

Figure 4.14 Output for the case of increase of 20% resistance

- **Case 6:** For increase of 50% of resistance, the change at the output of wheatstone bridge is 4.562mV and the output will be 198.4490mV having 43.5 gain from the difference amplifier. The offset for the output waveform is 480.1mV. The output waveform is given in Figure 4.15

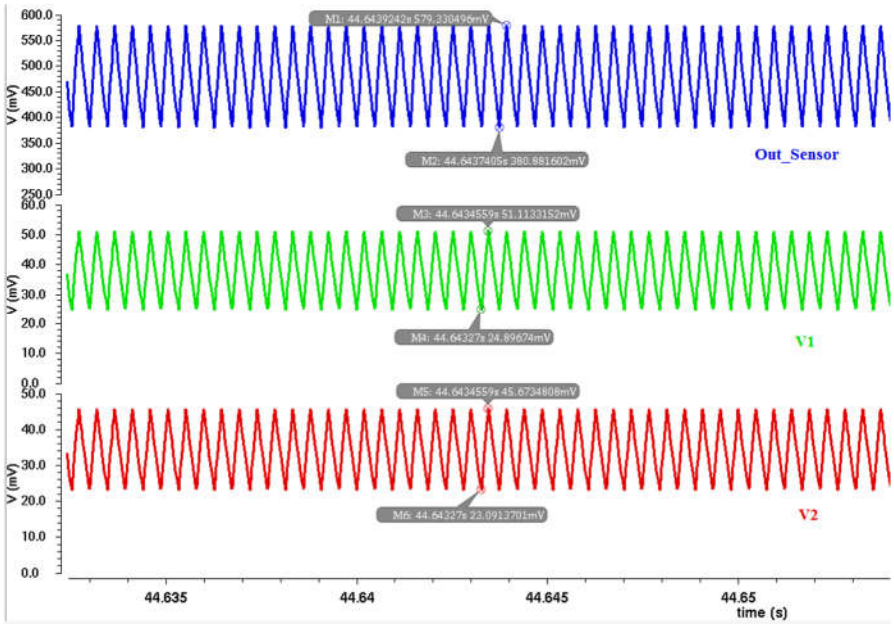

Figure 4.15 Output for the case of increase of 50% resistance

- **Case 7:** For increase of 100% of resistance, the change at the output of wheatstone bridge is 6.553mV and the output will be 285.097mV having 43.5 gain from the difference amplifier. The offset for the output waveform is 631.2mV. The output waveform is given in Figure 4.16

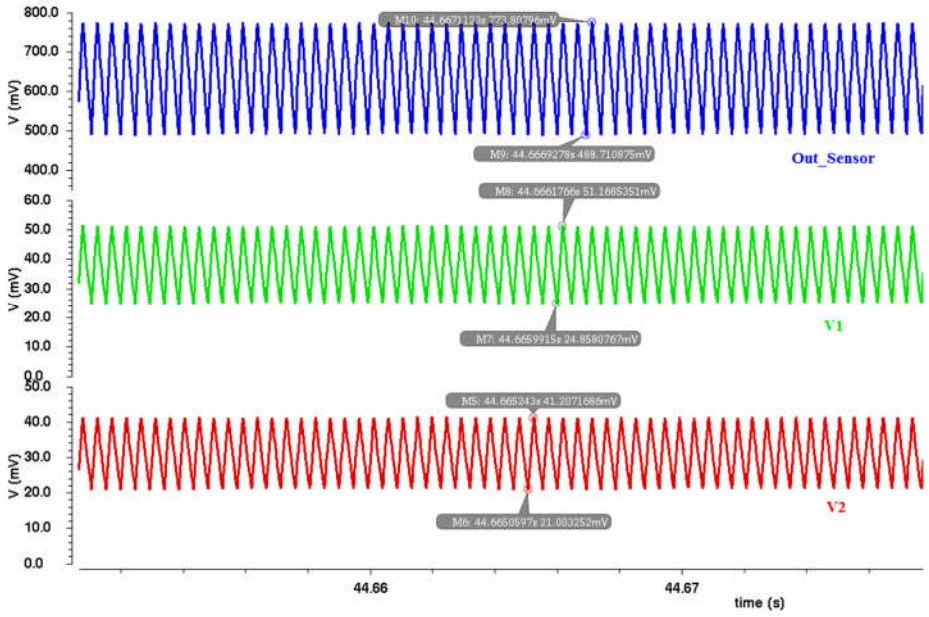

Figure 4.16 Output for the case of increase of 100% resistance

If the change of resistance occurs by decreasing the value of resistance, still we get the same relation with output being multiplied by the value of gain of difference amplifier. Two cases are discussed here just in order to depict the idea that resistance change in either direction will not affect the working of sensor. The only difference would be the offset which will increase in positive direction.

- **Case 8:** For decrease of 5% of resistance the resistance of gas sensitive resistor is 950Ω, the change at the output of wheatstone bridge is 0.579mV and the output will be 25.202mV having 43.5 gain from the difference amplifier. The offset for the output waveform is 178.5mV. The output waveform is given in Figure 4.17

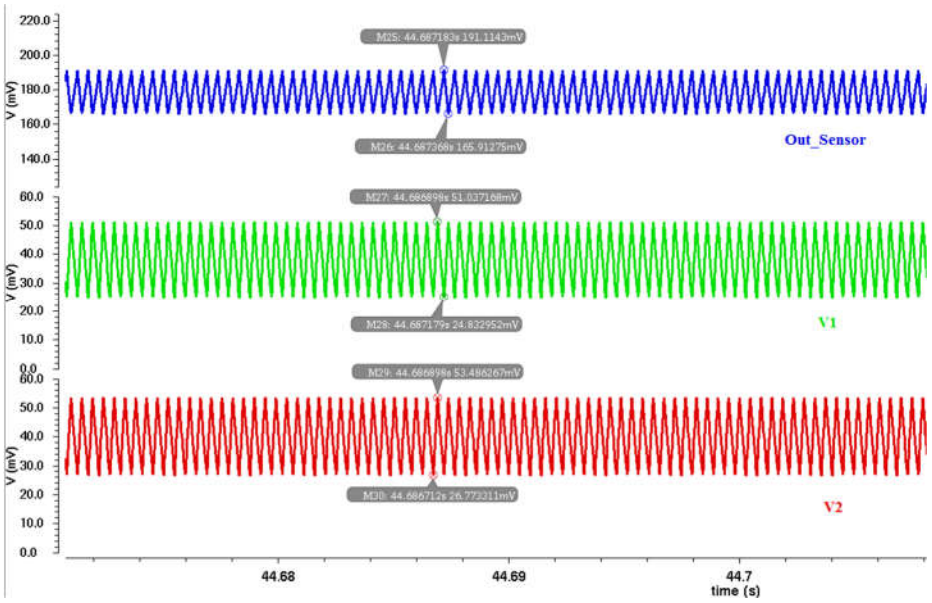

Figure 4.17 Output for the case of decrease of 5% resistance

- **Case 9:** For decrease of 10% of resistance the resistance of gas sensitive resistor is 900Ω, the change at the output of wheatstone bridge is 0.821mV and the output will be 35.720mV having 43.5 gain from the difference amplifier. The offset for the output waveform is 154.4mV. The output waveform is given in Figure 4.18

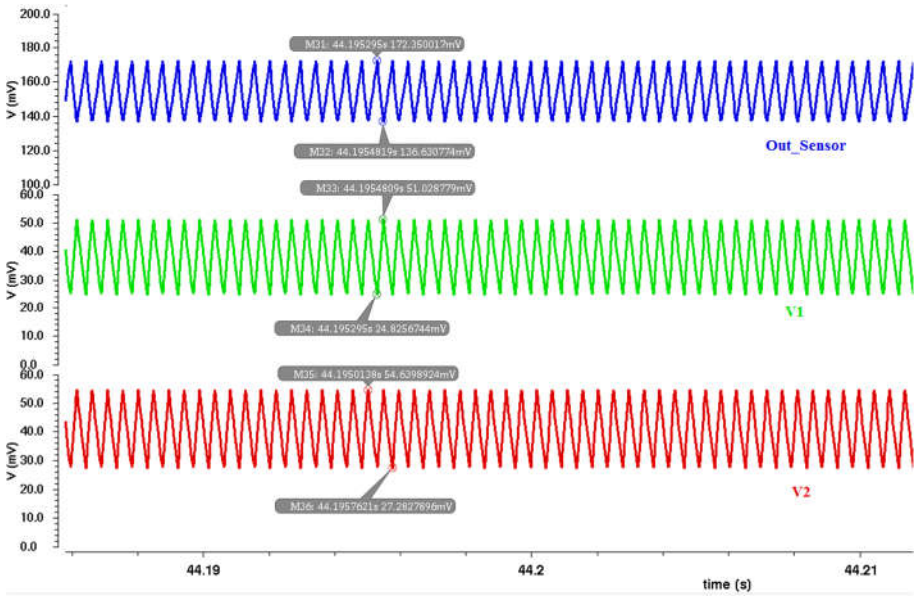

Figure 4.18 Output for the case of decrease of 10% resistance

Now for the cases when the resistance of micro-heater is in range of MΩ, so all the other resistors are chosen in MΩ and applied the same condition over the Wheatstone bridge to evaluate the performance of the sensor.

Case 1: When the bridge is constructed with MΩ resistors, we choose 1MΩ for both resistance for the normal resistors and 1MΩ for the micro-heater based resistors. When no gas is present, No change for the gas sensitive resistor takes place and both the outputs of Wheatstone bridge will have a little difference of offset as they are directly connected to difference amplifier but the amplitude will be same. The output for the difference amplifier will be a very small voltage due to common mode gain which is ideally zero but practically not. The output is around 2mV for the inputs of 26.182mV

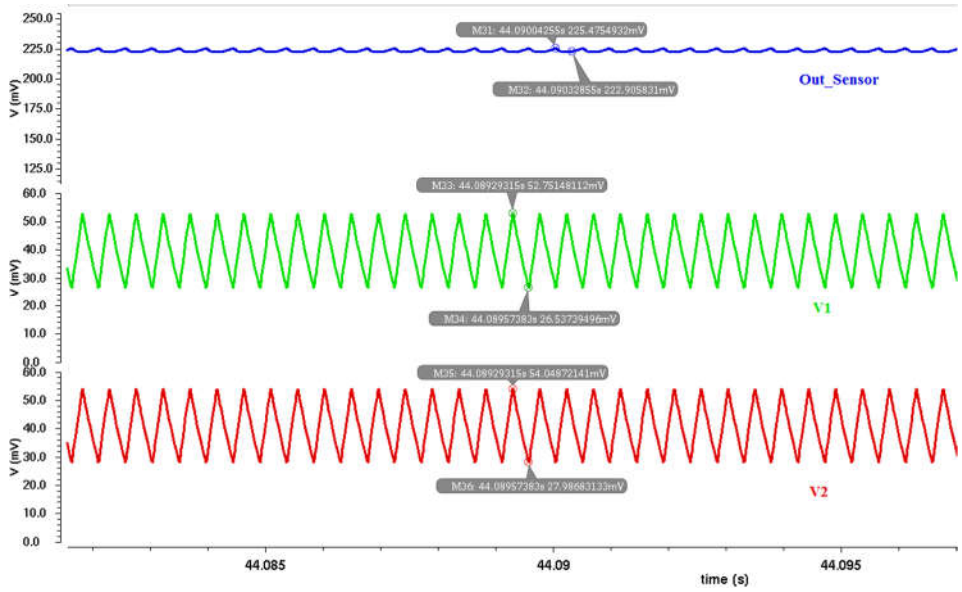

Figure 4.19 Output for the case 1MΩ - 1MΩ

- **Case 2:** When the gas is present and the resistance of the gas sensitive resistor starts to change. For increase of 1% of resistance, the change at the output of wheatstone bridge is 0.181mV and the output will be 7.897mV having 43.5 gain from the

difference amplifier. The offset for the output waveform is 216.3mV. The output waveform is given in Figure 4.20.

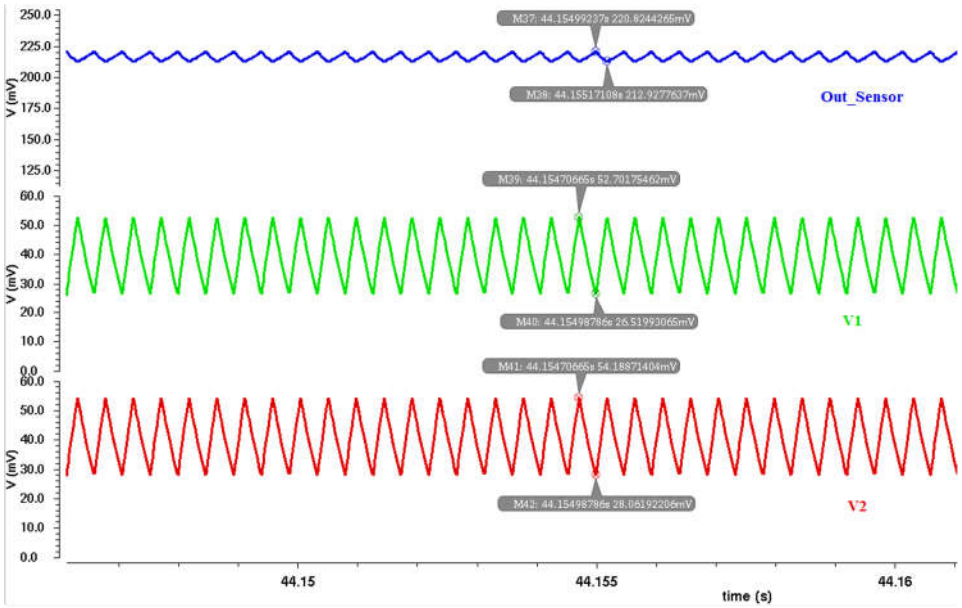

Figure 4.20 Output for the case of increase of 1% resistance

- **Case 3:** For increase of 5% of resistance, the change at the output of wheatstone bridge is 0.408mV and the output will be 17.77mV having 43.5 gain from the difference amplifier. The offset for the output waveform is 252.9mV. The output waveform is given in Figure 4.21

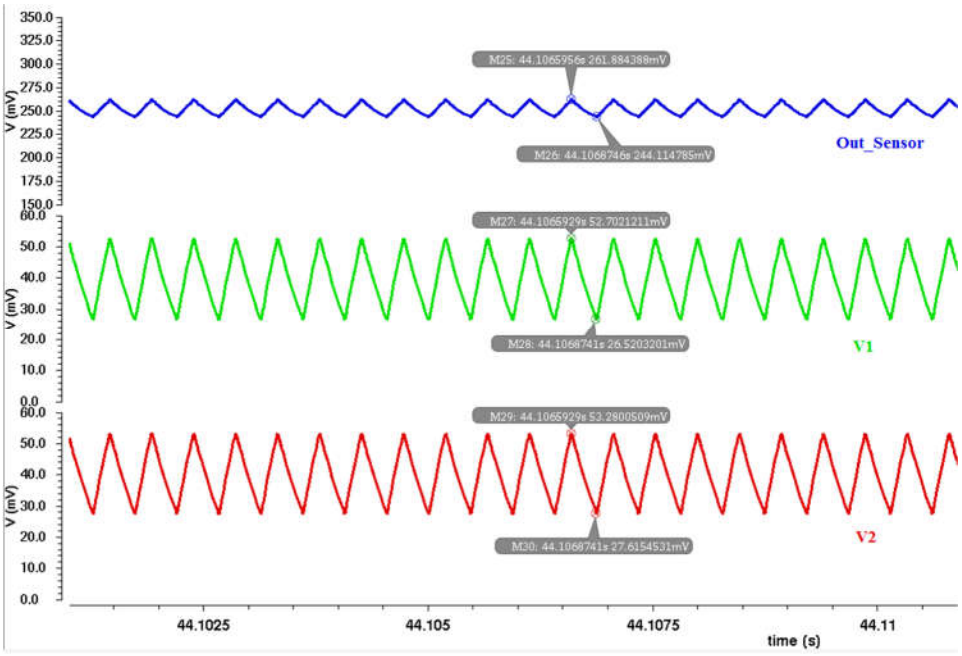

Figure 4.21 Output for the case of increase of 5% resistance

- **Case 4:** For increase of 10% of resistance, the change at the output of wheatstone bridge is 1.010mV and the output will be 43.942mV having 43.5 gain from the difference amplifier. The offset for the output waveform is 288.6mV. The output waveform is given in Figure 4.22

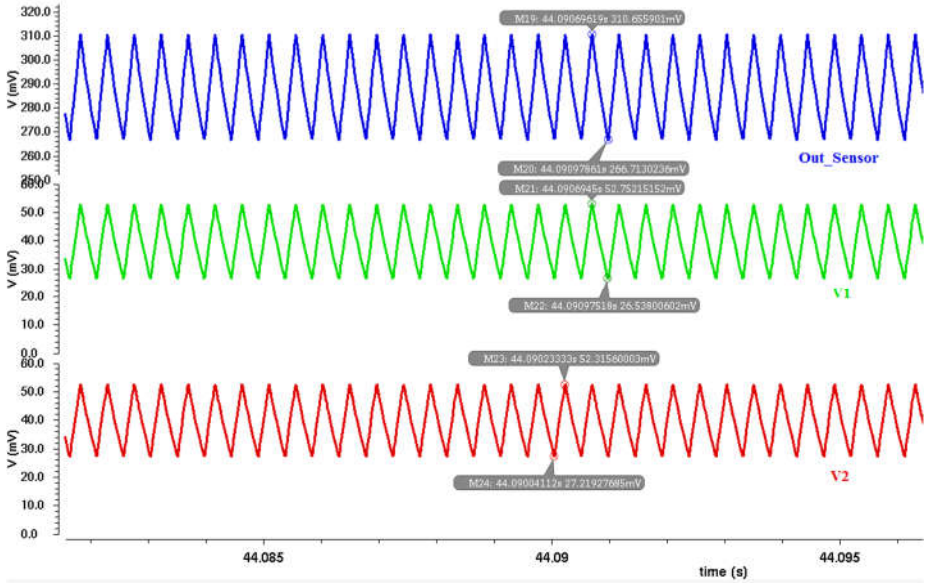

Figure 4.22 Output for the case of increase of 10% resistance

- **Case 5:** For increase of 20% of resistance, the change at the output of wheatstone bridge is 2.070mV and the output will be 90.050mV having 43.5 gain from the difference amplifier. The offset for the output waveform is 355.6mV. The output waveform is given in Figure 4.23.

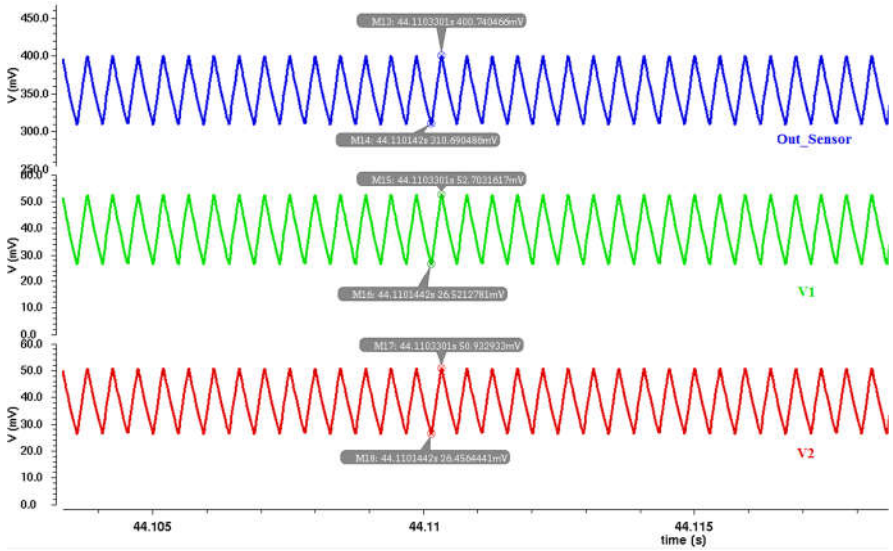

Figure 4.23 Output for the case of increase of 20% resistance

- **Case 6:** For increase of 50% of resistance, the change at the output of wheatstone bridge is 4.719mV and the output will be 205.288mV having 43.5 gain from the difference amplifier. The offset for the output waveform is 517.1mV. The output waveform is given in Figure 4.24

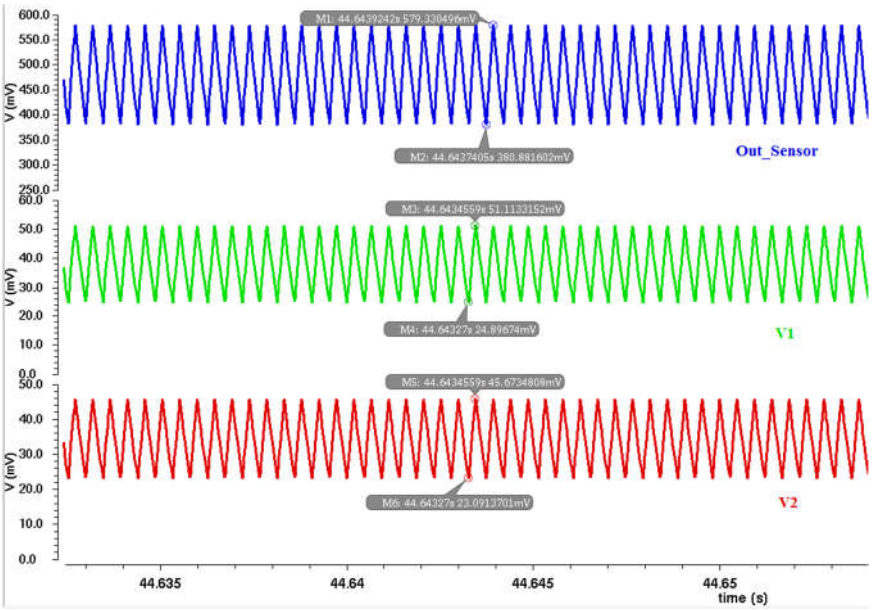

Figure 4.24 Output for the case of increase of 50% resistance

- **Case 7:** For increase of 100% of resistance, the change at the output of wheatstone bridge is 6.340mV and the output will be 275.79mV having 43.5 gain from the difference amplifier. The offset for the output waveform is 679.4mV. The output waveform is given in Figure 4.25

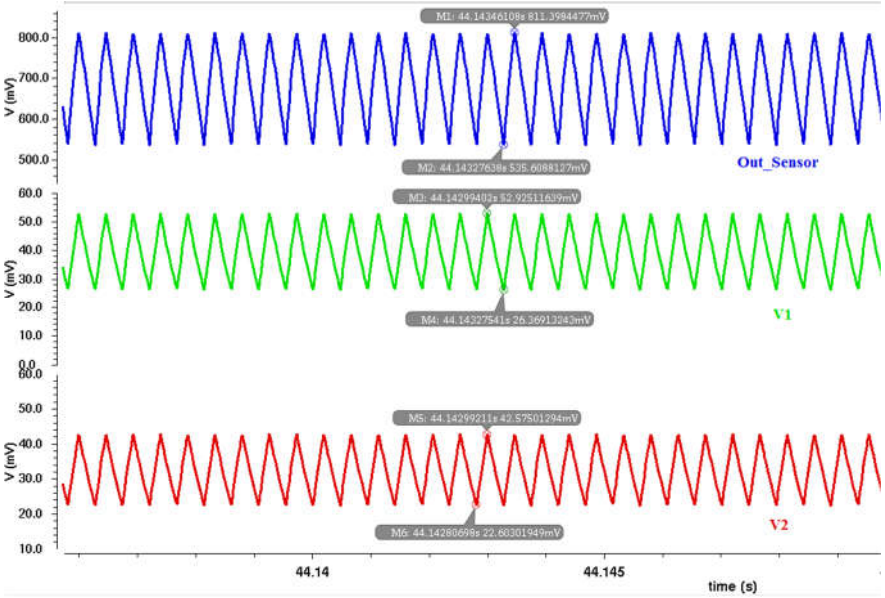

Figure 4.25 Output for the case of increase of 100% resistance

If the change of resistance occurs by decreasing the value of resistance, still we get the same relation with output being multiplied by the value of gain of difference amplifier. Two cases are discussed here just in order to depict the idea that resistance change in either direction will not affect the working of sensor. The only difference would be the offset which will increase in positive direction.

- **Case 8:** For decrease of 5% of resistance the resistance of gas sensitive resistor is 950KΩ, the change at the output of wheatstone bridge is 0.631mV and the output will be 27.476mV having 43.5 gain from the difference amplifier. The offset for the output waveform is 187.1mV. The output waveform is given in Figure 4.26

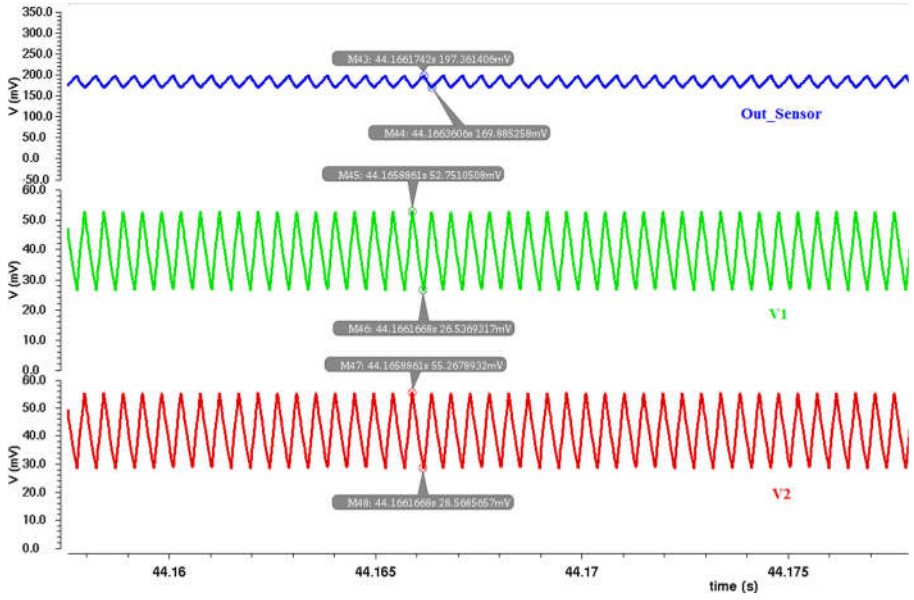

Figure 4.26 Output for the case of decrease of 5% resistance

- **Case 9:** For decrease of 10% of resistance the resistance of gas sensitive resistor is 900KΩ, the change at the output of wheatstone bridge is 0.871mV and the output will be 37.923mV having 43.5 gain from the difference amplifier. The offset for the output waveform is 156.8mV. The output waveform is given in Figure 4.27

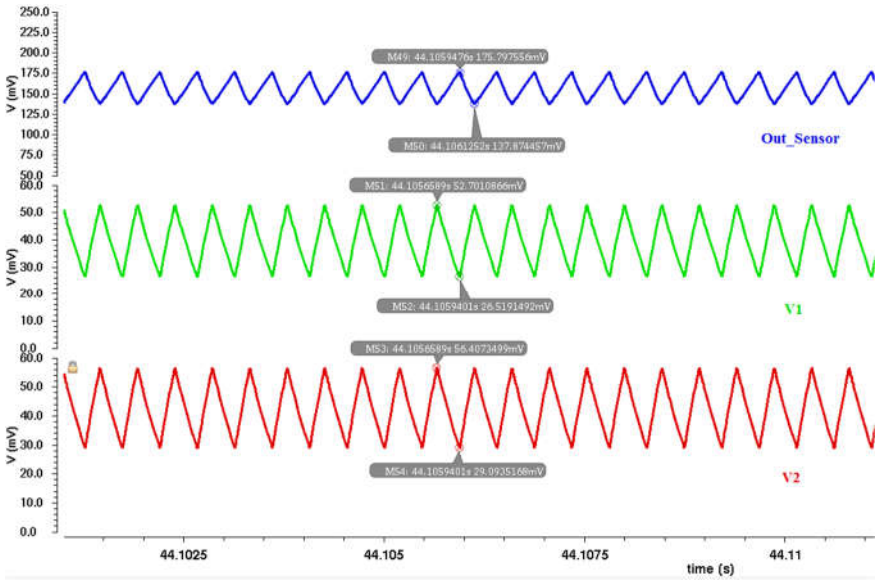

Figure 4.27 Output for the case of decrease of 10% resistance

4.7 Summary of the Results

The results can be summarized in the following tables. For the increase of resistance in the range of KΩ, the results are as follows

Table 4.1 Summary for increase in Resistance of KΩ

Resistor values (Ω)	% change	V1 on bridge (mV)	V2 on bridge (mV)	Output of Wheatstone bridge (mV)	Output voltage of Sensor (mV)	Gain	Offset voltage (mV)
1K-1.01K	1	26.205	26.080	0.125	5.439	43.5	207.3
1K-1.05K	5	26.207	25.774	0.433	18.854	43.5	240.2
1K-1.1K	10	26.278	25.270	1.008	43.535	43.5	272.3
1K-1.2K	20	26.211	24.143	2.068	90.001	43.5	332.7
1K-1.5K	50	26.217	21.655	4.562	198.449	43.5	480.1
1K-2K	100	26.310	19.757	6.553	285.097	43.5	631.2

If the change results in decrease of resistance, the circuit will work fine as well, we just tested two conditions in order to make sure the circuit works perfectly. The offset in this situation will increase positively with the decrease of voltage. The following table shows the results for change of 5% and 10% decrease in the given value.

Table 4.2 Summary of decrease of resistance in KΩ

Resistor values (Ω)	**% change**	**V1 on bridge (mV)**	**V2 on bridge (mV)**	**Output of Wheatstone bridge (mV)**	**Output voltage of Sensor (mV)**	**Gain**	**Offset voltage (mV)**
1K-950	5	26.205	26.784	0.579	25.202	43.5	178.5
1K-900	10	26.203	27.024	0.821	35.720	43.5	154.4

For the results of MΩ the table summarize the findings as

Table 4.3 Summary of increase in resistance in MΩ

Resistor values (Ω)	**% change**	**V1 on bridge (mV)**	**V2 on bridge (mV)**	**Output of Wheatstone bridge (mV)**	**Output voltage of Sensor (mV)**	**Gain**	**Offset voltage (mV)**
1M-1.01M	1	26.182	26.001	0.181	7.897	43.5	216.3
1M-1.05M	5	26.182	25.774	0.408	17.77	43.5	252.9
1M-1.1M	10	26.214	25.204	1.010	43.942	43.5	288.6
1M-1.2M	20	26.190	24.112	2.070	90.050	43.5	355.6
1M-1.5M	50	26.210	21.495	4.719	205.288	43.5	517.1
1M-2M	100	26.556	20.216	6.340	275.790	43.5	679.4

For the decrease in resistance in this case, we again checked two cases to make sure the working of the sensor. Summary is given in table below

Table 4.4 Summary of decrease in resistance for MΩ

Resistor values (Ω)	% change	V1 on bridge (mV)	V2 on bridge (mV)	Output of Wheatstone bridge (mV)	Output voltage of Sensor (mV)	Gain	Offset voltage (mV)
1M-950K	5	26.215	26.846	0.631	27.476	43.5	187.15
1M-900K	10	26.190	27.061	0.871	37.923	43.5	156.8

The Following graph shows the change of resistance for sensing resistor against the output of the Wheatstone bridge in differential mode.

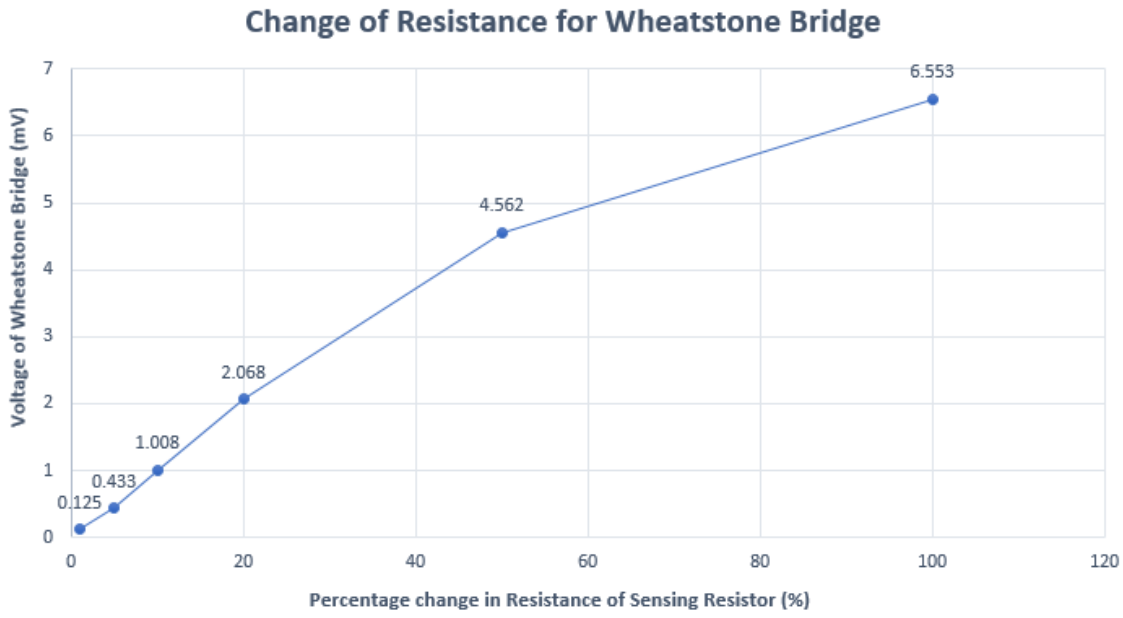

Figure 4.28 Change of resistance for Wheatstone bridge

The output of sensor for the change of resistance is given by the following graph

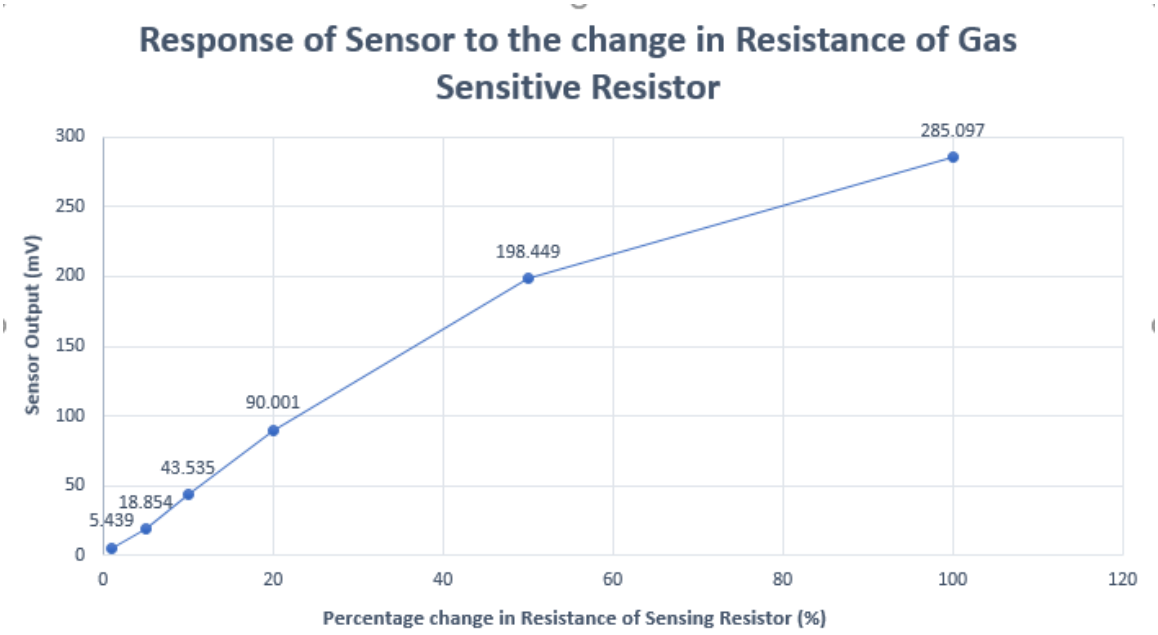

Figure 4.29 Response of Sensor to the change in resistance of gas sensitive resistor

4.8 Comparison with Other Sensors:

The comparison of wireless gas sensor with the available solutions is summarized in the table below. Our gas sensor is without the transmission block only while performing all the other tasks till the output. If we use the same radio module DD2 ETRX357 ZigBee transceiver used by the Somov [8] , which have power consumption of 31mW and average power consumption of 1.03mW we will still be consuming less power consumption as compared to others. The following table gives the comparison of the recent gas sensors.

Table 4.5 State-of-the-art Gas Sensing Circuits: Comparative Study

	Ho[26]	Wobscholl [27]	FlyPort [28]	Somov [29]	Yokosawa [30]	Somov [31]	Somov [1]	This Work
Year	2007	2006	2013	2011	2008	2012	2014	2017
Application	Hazardous gases detection	Toxic gases monitoring	LPG, natural gas	Combustible gases monitoring	Hydrogen monitoring	Hazardous gases detection	Hazardous gases detection	Hazardous gases detection
Sensing Power Consumption	1550mW	250mW for Circuit, 1000mW for Micro heater; 1250mW (complete sensor)	800mW for the microheater module	120mW for Circuit, 264mW for Micro heater; 384mW (complete sensor)	40mW for Circuit, 200mW for Micro heater; 240mW (complete sensor)	124.30mW for Circuit, 113mW for Micro heater; 238.18mV (complete sensor)	7.4mW for Circuit, 85.68mW for Micro heater; 93.08mW (complete sensor)	38.77µW without microheater; Expected power 2.5mW (complete sensor)
Heating Time	N/A	2sec	0.5sec	1 sec	1 sec	0.7sec	0.3sec	2sec (for possible worst case)
Sensitivity (full scale variation)	N/A	0.38V for 133% increase	Dependent on MCU	0.8V for 120% increase	0.4V	0.4V	30mV for W.B 6mV for differential	285mV for 100% increase
Sensor front end	Laser spectroscopic	Semiconductor/ Catalytic	Semiconductor	Semiconductor	FET	Catalytic	Catalytic	Semiconductor/ Catalytic

Comparing with the least power consumption, The Somov [8] gas sensor has a full range of sensitivity 30mV in Wheatstone bridge configuration and 6mV in differential configuration when the resistance changes to full scale. With this work, the 30mV difference is achieved with only 5% of resistance change and the full-scale change of 470mV is available with 5.06mV change with only 1% of resistance change.

CHAPTER 5

POST LAYOUT SIMULATION

The post layout simulations of the proposed Schmitt trigger, the sensor circuit based on proposed Schmitt trigger and sensor circuit based on proposed Schmitt trigger is done in this last chapter. This chapter outlines the layout of the proposed design and how simulations are affected after layout extraction.

5.1 Layout for gas sensor circuit based on Schmitt Trigger based Timer.

The layout is created in order to make the sensor universal and to be used for any gas with the requirements suitable for any user. For this purpose, the capacitors of both sub-hertz and 1 KHz is placed off-chip so that it can be used according to requirement of designer. The Wheatstone bridge containing the microheaters will also be off chip and the resistors for deciding the gain of the difference amplifier at the end will also be off chip in order to give the flexibility to the designer to select those values according to the requirements. The layout for the chip is shown in Figure 5.1

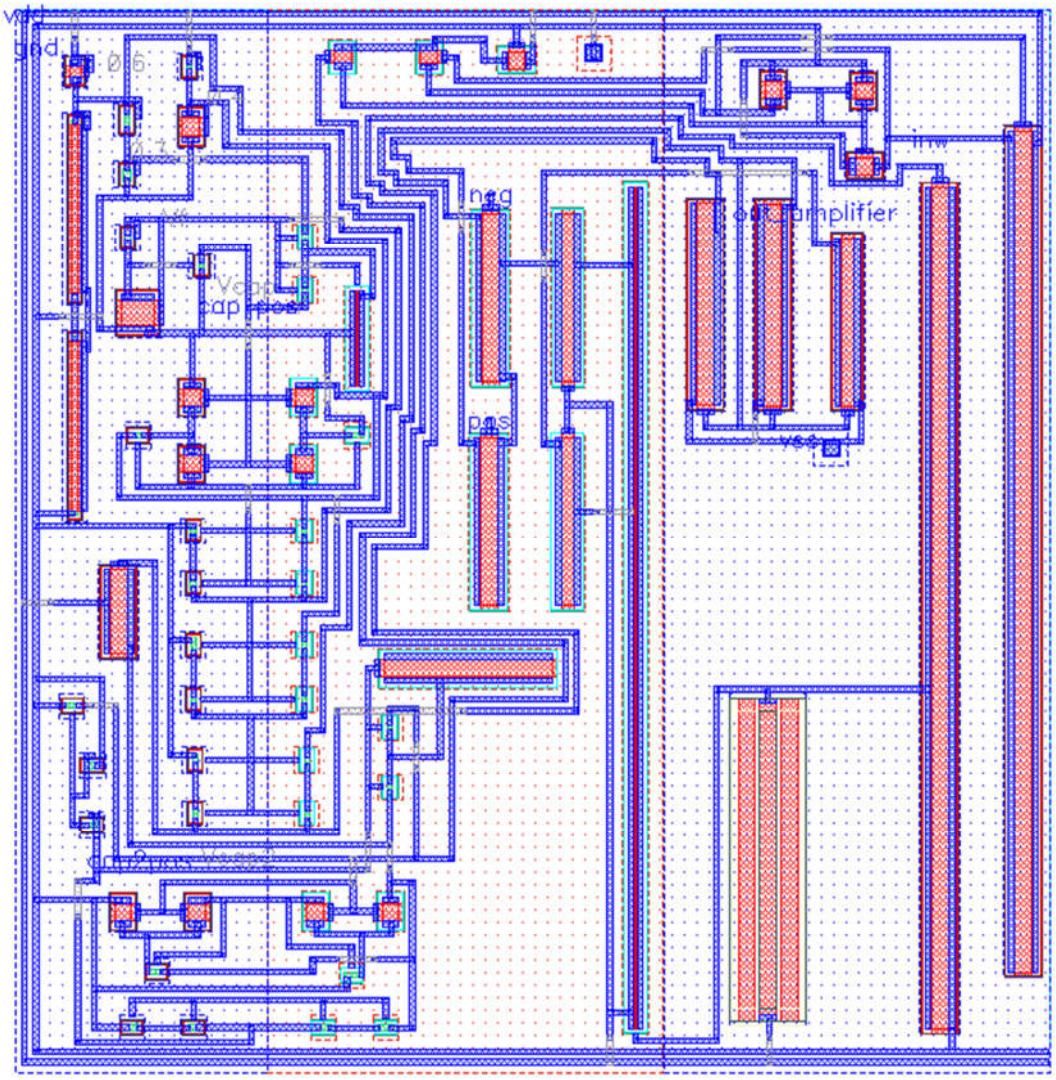

Figure 5.1 Layout for first configuration of the gas sensor **(layout floorplanning)**

5.2 Post Layout Simulations for both configuration of gas sensors

The post layout simulation is for the configuration is given in Figure 5.2. There is small difference in the value of output voltage due to parasitic in connection.

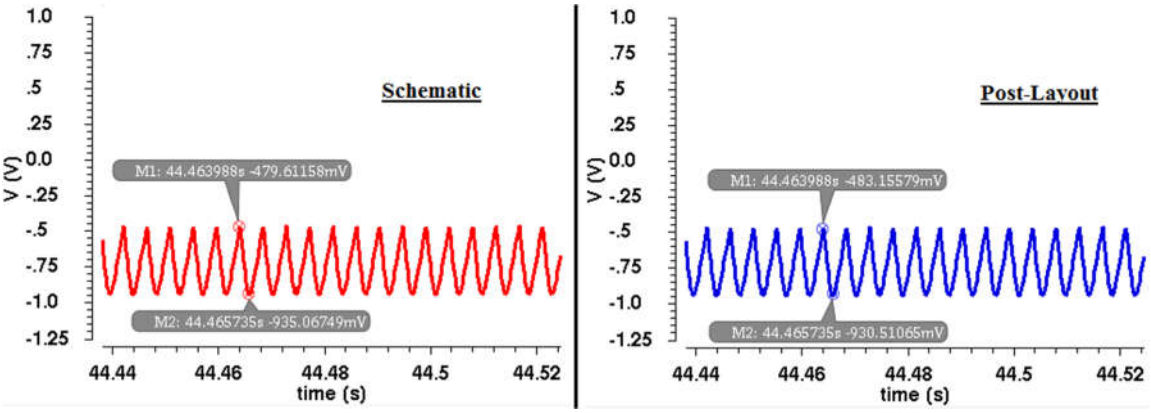

Figure 5.2 Comparison of schematic and post-layout simulation for first configuration

The results for the post layout and schematic are compared in the table 5.2. There is small difference due to parasitic in the connections of extracted version.

Table 5.1 Comparison for both configurations

Configurations	Schematic	Post-layout
1 Output (mv)	455.456	448.351

CHAPTER 6

CONCLUSION AND FUTURE WORK

In this chapter, the conclusion and inferences of the thesis are summarized. This mainly outlines the considered problem, the proposed solution and analysis of the results. Also, a discussion on the prospects of extending this work in future is presented at the end.

6.1 Conclusion

The purpose of this work is to design a Wireless gas sensor with lower power consumption then the available solutions while keeping the sensitivity of the sensor. The idea was to avoid the use of microcontroller and use the sub hertz oscillator and circuit techniques in order to achieve the purpose of gas sensing smartly. The first objective was the reduction of power consumption for the whole sensor which is achieved by making the circuit level implementation of required blocks for the operation and then optimizing them to get the required results. A new approach of integrated sensor is achieved instead of using microcontroller and other blocks for the sensors. The next target was keeping the sensitivity comparable while going down in power consumption. We have improved the sensitivity of the wireless sensor by using a high gain difference amplifier at the end which uses average power of 3.2μW but provides the gain of 63.5 which makes the output range of 470mV for full scale variation. This allowed us to take the measurement just when the resistance starts changing around 200°C [5] instead of going to higher temperatures. This will reduce sufficiently the amount of power significantly as more power is lost in the heating of the gas sensor. The average power consumption of the whole circuit is 38.77μW without the

micro-heater power consumption. The commercial micro-heater CCS801 by Cambridge CMOS Sensors will consume 1mW average power for our time of operation and including DD2 ETRX357 ZigBee transceiver block for transmission will add another 1mW average power which will combine to give 2.072mW as overall for the whole sensor which is still very less with the available solutions.

6.2 Future Work:

This work can be continued with the fabricating the design to make the chip of this wireless gas sensor. Furthermore, the micro-heater with suitable materials can also be fabricated on to the single chip to make the wireless gas sensor fully integrated. The effect of heat would be studied and how to shield the other parts of circuit from this heat if micro-heater is located on the same chip. After fabrication, the testing can be performed and the results will be analyzed. With more than one wireless sensors, a wireless sensor network will be created in order to monitor various areas of the industry. The same sensor with different operating time can be used according to the conditions of that place. If the place has human life working then sensors can take the measurements after a short interval of time and for the other places like gas pipelines outside the industry, the reading time can be made maximum in order to reduce the average power and increase the life of wireless sensor batteries.

References

[1] Mohamed Hefeeda and Majid Bagheri," Wireless Sensor Networks for Early Detection of Forest Fires", International Conference on Mobile Adhoc and Sensor Systems, 2007, 8-11 Oct. 2007, Pisa, Italy, IEEE, Page(s): 1- 6

[2] Xiao Liu, Sitian Cheng, Hong Liu, Sha Hu, Daqiang Zhang and Huansheng Ning," A Survey on Gas Sensing Technology", 28 Oct - 31 Oct 2012, Taipei, Taiwan, Page(s): 9635-9665; doi:10.3390/s120709635.

[3] Stefano Tranquillini, Patrik Spieß, Florian Daniel, Stamatis Karnouskos, Fabio Casati, Nina Oertel, Luca Mottola, Felix Jonathan Oppermann, Gian Pietro Picco, Kay Römer, Thiemo Voigt," Process-Based Design and Integration of Wireless Sensor Network Applications", Lecture Notes in Computer Science Volume 7481, 2012, Berlin, Heidelberg pp 134-149. DOI: 10.1007/978-3-642-32885-5_10

[4] G. N. L. Ravi Teja, V. K. R. Harish, Nayeem Muddin Khan D, R. Bhargava Krishna, Rajesh Singh, S Chaudhary," Land Slide Detection and Monitoring System using Wireless Sensor Networks (WSN)", IEEE International Advance Computing Conference (IACC), 21-22 Feb. 2014, Gurgaon, India, DOI: 10.1109/IAdCC.2014.6779310.

[5] Luís M. L. Oliveira, Joel J. P. C. Rodrigues," Wireless Sensor Networks: A Survey on Environmental Monitoring", Journal of Communications, VOL. 6, No. 2, April 2011.

[6] Jonathan Isaac Chanin Andrew R. Halloran," Wireless Sensor Network for Monitoring Applications", A Major Qualifying Project Report Submitted to the University of Worcester Polytechnic Institute, October 2003.

[7] Gang Zhao," Wireless Sensor Networks for Industrial Process Monitoring and Control: A Survey", Network Protocols and Algorithms ISSN 1943-3581, Vol. 3, No. 1, 2011. DOI: https://doi.org/10.5296/npa.v3i1.580

[8] Andrey Somov, Alexander Baranov, Denis Spirjakin, and Roberto Passerone," Circuit Design and Power Consumption Analysis of Wireless Gas Sensor Nodes: One-Sensor Versus Two-Sensor Approach", IEEE Sensors Journal, Vol. 14, NO. 6, June 2014. Page(s): 2056 – 2063 DOI: 10.1109/JSEN.2014.2309001

[9] A. Somov, A. Baranov, A. Savkin, D. Spirjakin, A. Spirjakin, and R. Passerone, "Development of Wireless Sensor Network for Combustible Gas Monitoring," Sens. Actuators A, Phys., vol. 171, no. 2, pp. 398–405, Jul. 2011.

[10] Kavi K. Khedo, Rajiv Perseedoss and Avinash Mungur, "A Wireless Sensor Network Air Pollution Monitoring System", International Journal of Wireless and Mobile Networks (IJWMN), Vol 2, No 2, May 2010.

[11] Jer Hayes, Stephen Beirne, King-Tong Lau, Dermot Diamond," Evaluation of a low cost Wireless Chemical Sensor Network for Environmental Monitoring", IEEE Sensors, 26-29 Oct. 2008, Lecce, Italy, DOI: 10.1109/ICSENS.2008.4716494

[12] S.E. Moon, H.-K. Lee, N.-J. Choi, J. Lee, C.A. Choi, W.S. Yang, J. Kim, J.J. Jong, D.-J. Yoo," Low power consumption micro C2H5OH gas sensor based on micro-heater and screen printing technique", Sensors and Actuators B 187 (2013) Page(s): 598– 603.

[13] J. Hayes, S. Beirne, K.-T. Lau, and D. Diamond, “Evaluation of a low cost wireless chemical sensor network for environmental monitoring,” in Proc. Sensors, 2008, pp. 530–533.

[14] I.F. Akyildiz, W. Su, Y. Sankarasubramaniam, E. Cayirci,” Wireless sensor networks: a survey” Elseveir Journal on Computer Networks Volume 38, Issue 4, 15 March 2002, Pages 393–422.

[15] AMA association for sensor technology, Europe, “Trends in Future-Oriented Sensor Technologies”, July 2010.

[16] Dan Chen, Zhixin Liu, Lizhe Wang, Minggang Dou, Jingying Chen, Hui Li,” Natural Disaster Monitoring with Wireless Sensor Networks: A Case Study of Data-intensive Applications upon Low-Cost Scalable Systems” Mobile Networks and Applications October 2013, Springer, Volume 18, Issue 5, pp 651-663.

[17] B O’Flynn, Rafael Martínez, Català, S. Harte, C. O’Mathuna, John Cleary, C. Slater, F. Regan, D. Diamond, Heather Murphy,” SmartCoast: A Wireless Sensor Network for Water Quality Monitoring”, 32nd IEEE Conference on Local Computer Networks. 15-18 Oct. 2007, Dublin, Ireland, DOI: 10.1109/LCN.2007.34

[18] Liqun Hou and Neil W. Bergmann,” Novel Industrial Wireless Sensor Networks for Machine Condition Monitoring and Fault Diagnosis”, IEEE Transactions on Instrumentation and Measurement, Vol. 61, NO. 10, October 2012. Page(s): 2787 - 2798

[19] A. Somov et al., “Energy-Aware Gas Sensing Using Wireless Sensor Networks” (Lecture Notes in Computer Science). New York, NY, USA: Springer-Verlag, 2012, pp. 245–260.

[20] S. Ho, F. Koushanfar, A. Kosterev, and F. Tittel, “LaserSPECks: Laser spectroscopic trace-gas sensor networks-sensor integration and application,” in Proc. IPSN, 25-27 April 2007, Cambridge, MA, USA, pp. 226–235

[21] Seokhyeon Jeong, Zhiyoong Foo, Yoonmyung Lee, Jae-Yoon Sim, David Blaauw and Dennis Sylvester,” A Fully-Integrated 71 nW CMOS Temperature Sensor for Low Power Wireless Sensor Nodes”, IEEE Journal of Solid-State Circuits, Vol. 49, No. 8, August 2014 Page(s): 1682 – 1693.

[22] Shailesh Singh Chouhan and Kari Halonen,” A Low Power Temperature to Frequency Converter for the On-Chip Temperature Measurement”, IEEE Sensors Journal, Vol. 15, NO. 8, August 2015. Page(s): 4234 - 4240

[23] W. Chen, G. Liu, B. Zdravko, and A. M. Niknejad, “A highly linear broadband CMOS LNA employing noise and distortion cancellation,” IEEE J. Solid-State Circuits, vol. 43, no. 5, pp. 1164–1176, May 2008.

[24] Dake Wu, Ru Huang, Waisum Wong, and Yangyuan Wang, “A 0.4-V Low Noise Amplifier Using Forward Body Bias Technology for 5 GHz Application”, IEEE Microwave and Wireless Components Letters, Vol. 17, NO. 7, July 2007. Page(s): 543 - 545

[25] (2013). Flyport Sensing Platform [Online]. Available: http://www.openpicus.com

[26] Akira Shikata, Ryota Sekimoto, Tadahiro Kuroda and Hiroki Ishikuro," A 0.5 V 1.1 MS/sec 6.3 fJ/Conversion-Step SAR-ADC With Tri-Level Comparator in 40 nm CMOS", IEEE Journal of Solid-State Circuits, Vol. 47, No. 4, April 2012.

[27] Poki Chen, Chun-Chi Chen, Yu-Han Peng, Kai-Ming Wang, and Yu-Shin Wang," A Time Domain SAR Smart Temperature Sensor with Curvature Compensation and a 3σ Inaccuracy of 0.4 C ~ +0.6 C Over a 0 C to 90 C Range", IEEE Journal of Solid-State Circuits, Vol. 45, No. 3, March 2010.

[28] Adel S. Sedra, Kenneth C. Smith "Microelectronic Circuits" Oxford Series in Electrical & Computer Engineering, 6th Edition.

[29] Yu-Shiang Lin, Dennis Sylvester and David Blaauw," A sub-pW timer using gate leakage for ultra-low-power sub-Hz monitoring systems", IEEE Custom Integrated Circuits Conference (CICC) 16-19 Sept. 2007, San Jose, CA, USA

[30] Product brief for CCS801, Ultra-low power multi-gas sensor for indoor air quality, Cambridge CMOS Sensors.

[31] M. Baroncini, P. Placidi, G.C. Cardinali, A. Scorzoni," Thermal characterization of a microheater for micromachined gas sensors", Sensors and Actuators Volume 115, Issue 1, 15 September 2004, Pages 8–14

[32] S. Vallejos, I. Gràcia E. Figueras, J. Sánchez, R. Mas, O. Beldarrain, C. Cané, "Microfabrication of flexible gas sensing devices based onnanostructured semiconducting metal oxides", Sensors and Actuators A Volume 219, 1 November 2014, Pages 88–93.

[33] G.Velmathi, S.Mohan , N.Ramshanker, “Importance of Temperature in Gas Sensors and Design, Fabrication, Testing of S shaped Low Power Platinum Microheater for Gas Sensor Applications”, International Journal of Emerging Trends in Electrical and Electronics, Vol. 5, Issue. 2, July-2013.

[34] M. A. Khan, G. Dumstorff, C. Winkelmann, W. Lang,” Investigations on Noise Level in AC- and DC- Bridge circuits for sensor measurement systmes”, GMA/ITG-Fachtagung Sensoren und Messsysteme 2016

[35] C. O. Mathuna, T. O’Donnell, R. V. Martinez-Catala, J. Rohan, and B. O’Flynn, “Energy scavenging for long-term deployable wireless sensor networks,” Talanta J., vol. 75, no. 3, pp. 613–623, May 2008.

[36] M. Cihan Çakır, Deniz Çalı¸skan , Bayram Bütün and Ekmel Özbay,” Planar Indium Tin Oxide Heater for Improved Thermal Distribution for Metal Oxide Micromachined Gas Sensors”, Sensors 2016

[37] Mengying Zhang, Lidong Du, Zhen Fang and Zhan Zhao,” A Sensitivity-Enhanced Film Bulk Acoustic Resonator Gas Sensor with an Oscillator Circuit and Its Detection Application” Micromachines 2017, 8(1), 25; doi:10.3390/mi8010025

[38] D. Wobscholl, “A wireless gas monitor with IEEE 1451 protocol,” inProc. SAS, 2006, pp. 162–164.

[39] D. Kelaidonis et al., “Virtualization and cognitive management of real world objects in the internet of things,” in Proc. GreenCom, 2012, pp. 187–194.

[40] K. Yokosawa, K. Saitoh, S. Nakano, Y. Goto, and K. Tsukada, “FET hydrogen-gas sensor with direct heating of catalytic metal,” Sens. Actuators B, Chem., vol. 130, no. 1, pp. 94–99, Mar. 2008.

[41] Pratchayaporn Singhanath, Apirak Suadet, Arnon Kanjanop, Thawatchai Thongleam, Sanya Kuankid and Varakorn Kasemsuwan,” Low Voltage Adjustable CMOS Schmitt Trigger” 4th International Conference on Modeling, Simulation and Applied Optimization (ICMSAO), 19-21 April 2011, Kuala Lumpur, Malaysia

[42] Fei Yuan,” A high-speed differential CMOS Schmitt trigger with regenerative current feedback and adjustable hysteresis”, Mixed Signal Letter, Analog Integrated Circuits and Signal Process, Springer, Volume 63 Issue 1, April 2010 Pages 121 - 127

[43] Fei Yuan,” Differential CMOS Schmitt trigger with tunable hysteresis”, Express Letter, Analog Integrated Circuits and Signal Process, Springer, Volume 62 Issue 2, February 2010, Pages 245 – 248.

[44] Zhenhua Wang,” CMOS Adjustable Schmitt Triggers” IEEE Transactions on Instrumentation and Measurement, vol. 40. No. 3. June 1991. Page(s): 601 - 605

[45] A. Pfister,” Novel CMOS Schmitt Trigger with Controllable Hysteresis” Electronics Letters 26th March 1992 Vol. 28 No. 7 Page(s): 639 - 641

Vitae

Name	:Hamza Shahid
Nationality	:Pakistani
Date of Birth	:8/23/1989
Email	:hamzashahid2010@yahoo.com
Address	:House No 342, Ali block, Bahria town, Lahore
Academic Background	:Electrical Engineer

Publications:

[C1] Hamza Shahid, Umais Tayyab, Hussain Alzaher, “A CMOS Timer Circuit with Pulse Width Modulation for Sub-hertz Monitoring Applications”, accepted in 14th International MultiConference on Systems, Signals & Devices (SSD), Marrakech, Morocco, March 2017.

[C2] Umais Tayyab, Hamza Shahid, Hussain Alzaher, “A Self-Biased Active Precision Rectifier for Energy Harvesting Systems”, accepted in 14th International Multi-Conference on Systems, Signals & Devices (SSD), Marrakech, Morocco, March 2017.